



UNIVERSIDADE D
COIMBRA

Francisco André dos Santos Cruz

**DESIGN OF THE STRUCTURE OF A
LIGHTWEIGHT ROBOTIC MANIPULATOR**

Dissertação no âmbito do Mestrado Integrado em Engenharia Mecânica no ramo de Produção e Projeto, orientada pelo Professor Doutor Pedro Mariano Simões Neto e pelo Professor Doutor Mohammad Safeea e apresentada ao Departamento de Engenharia Mecânica da Faculdade de Ciências e Tecnologia da Universidade de Coimbra.

Julho de 2021

1 2



9 0

FACULDADE DE
CIÊNCIAS E TECNOLOGIA
UNIVERSIDADE DE
COIMBRA

Design of the structure of a lightweight robotic manipulator

Submitted in Partial Fulfilment of the Requirements for the Degree of Master in Mechanical Engineering in the speciality of Production and Project.

Projeto da estrutura de um manipulador robótico

Author

Francisco André dos Santos Cruz

Advisors

Pedro Mariano Simões Neto

Mohammad Safeea

Jury

President Professor Doutor José Luís Ferreira Afonso
Professor Auxiliar da Universidade de Coimbra

Vowels Professor Doutor Mohammad Safeea
Professor Convidado da Universidade de Coimbra
Professor Doutor Paulo Joaquim Antunes Vaz
Professor Adjunto do Instituto Politécnico de Viseu

Advisors Professor Doutor Pedro Mariano Simões Neto
Professor Auxiliar da Universidade de Coimbra
Professor Doutor Mohammad Safeea
Professor Convidado da Universidade de Coimbra

Coimbra, July, 2021

“Keep your eyes on the stars, and your feet on the ground.”

Theodore Roosevelt

Aos meus pais.

ACKNOWLEDGEMENTS

Reaching the end of this stage of my academic studies, it is time to express my deepest gratitude to all those who have made part of my journey.

First, the present work would never be possible without the full orientation, support, dedication, and availability of my advisors, Professor Doctor Pedro Neto and Professor Doctor Mohammad Safeea. To them, my highest appreciation for their patience and for the opportunity of working with them.

I am also hugely grateful to my colleagues in the laboratory, who were always ready to help. Thank you for your time, suggestions, and advice.

To my childhood, high school, and college friends, who have always supported me and with whom I share some of the best memories. Thanks for the laughs, for the talks, for the friendship. You are the reason why this journey was so pleasant.

Last but not least, to my family, but especially to my parents. For all the opportunities they gave me, for always supporting me, and for helping me conquer my dreams. I will never be able to thank them enough for everything they have done. Thank you, mom, and dad.

Abstract

In recent years, we have witnessed a great demand for machines that can perform tasks by themselves, especially robots. Nowadays, these devices are crucial for almost every modern production system and with the Fourth Industrial Revolution taking place, the interest in them (along with automation) only tends to increase. As a consequence, the requirements for current robots are also changing, as years go by. It is no longer enough to have robots that are exclusively designed to perform a single task, today, more than ever, versatility is the key. They must be capable of working alongside other robots or, in a more ideal scenario, operating in close collaboration with humans, which usually demands specified characteristics. Thereby, to satisfy the need for a type of robot that met those requirements, lightweight robots have been developed.

In this context, the motivation behind this work is to design and manufacture a compact lightweight robotic manipulator, with six degrees of freedom, at a low cost. The main target is to develop a fully functional prototype, with a kinematic redundancy similar to the human arm, that is capable of delivering high precision. The structural design and its optimization are the major subjects of this dissertation, which seeks to accomplish the best global performance possible while enhancing features such as high payload and low weight. Additionally, an easy-to-use and effective gesture-controlled user interface is also proposed, allowing a more intuitive experience for the operator.

Keywords Lightweight robots, Structural design, Dynamic simulation, Topology optimization, 3D printing.

Resumo

Nas últimas décadas, tem vindo a verificar-se um aumento exponencial na procura por mecanismos automatizados, especialmente robôs. Atualmente, estas máquinas desempenham um papel crucial na maioria dos sistemas produtivos modernos e com o crescente interesse quer pela digitalização, quer pela automação, resultante da revolução industrial em curso, é expectável que esta necessidade apenas tenda a aumentar. Desta forma, também os requisitos exigidos a um robô estão em constante mutação. Presentemente, torna-se muitas vezes pouco viável implementar um robô para desempenhar exclusivamente uma única tarefa, isto é, a versatilidade assume-se cada vez mais como um fator determinante. Assim, idealmente, um robô deverá ser capaz de operar em rede simultaneamente com outros robôs ou até, por vezes, em colaboração direta com o operador. De tal forma, para corresponder a este novo tipo de exigências, robôs com reduzida massa estrutural têm vindo a ser desenvolvidos.

Neste contexto, este projeto visa desenhar e fabricar um manipulador robótico de reduzida massa estrutural, com seis graus de liberdade e de baixo custo. O principal objetivo é construir um protótipo compacto, funcional, com uma redundância cinemática similar ao braço humano e que apresente elevada precisão. Nesse sentido, este trabalho incide essencialmente sobre o desenho estrutural e otimização do conjunto, procurando maximizar a capacidade de carga e minimizar o peso global do robô. Além disso, a interface de controlo é também considerada, sendo proposto um sistema de gestos intuitivo e de fácil utilização.

Palavras-chave: Robôs, Desenho estrutural, Simulação dinâmica, Otimização topológica, Impressão 3D.

Contents

LIST OF FIGURES	ix
LIST OF TABLES	xi
LIST OF SYMBOLS AND ACRONYMS	xiii
List of Symbols	xiii
Acronyms	xiii
1. INTRODUCTION.....	1
1.1. Problem and motivation	1
1.2. Proposed approach.....	2
1.3. Thesis overview	3
2. STATE OF THE ART.....	5
2.1. Design features of lightweight robots	6
2.2. Safety approach	10
2.3. Topology optimization.....	11
3. LIGHTWEIGHT ROBOT CONCEPT	15
3.1. Desirable characteristics.....	15
3.2. Design and drafting.....	16
4. STRUCTURAL DESIGN	19
4.1. Parts geometry	19
4.2. Torque analysis.....	21
4.3. Selection of the actuators	27
5. STRUCTURAL OPTIMIZATION.....	31
6. ROBOT MANUFACTURING.....	35
6.1. 3D printing	35
6.1.1. Printing parameters.....	35
6.2. Assembly process	36
7. EXPERIMENTS AND RESULTS	39
7.1. Precision.....	39
7.2. Payload.....	40
7.3. Control interface.....	40
8. CONCLUSIONS.....	43
8.1. Future work	43
BIBLIOGRAPHY.....	45
APPENDIX A (Manipulator technical drawings).....	49

LIST OF FIGURES

Figure 2.1. KUKA® LWR, the first commercialized version of the lightweight robot co-developed with <i>DLR</i>	7
Figure 2.2. The mechatronic joint design of the DLR-KUKA® LWR [6].....	9
Figure 2.3. COMPI robot from the <i>DFKI</i> [10].....	9
Figure 2.4. Comparative illustration of size, shape, and topology optimization [21].	11
Figure 2.5. Usual steps of topology optimization process [21].	12
Figure 2.6. Typical design process while using topology optimization [21].	13
Figure 3.1. Rough analysis of the predicted torque by sections.	17
Figure 4.1. Outcome concept design for the manipulator.	19
Figure 4.2. Illustration showing the perpendicular distance between the force (F) and the pivot point.	22
Figure 4.3. Illustration of the one-joint elementary assembly, showing 0 and 90-degree position.	22
Figure 4.4. Results for the one-joint elementary assembly, without considering gravity effect.	23
Figure 4.5. Analysis of the one-joint elementary assembly, considering gravity effect.	24
Figure 4.6. Illustration of the two-joint elementary assemble with indication of the first and second joints.....	24
Figure 4.7. Analysis of the two-joint assemble without (a) and with (b) gravitational effect.	25
Figure 4.8. Identification of the joints, as well as the forces which will be considered in the analysis.	25
Figure 4.9. Results given by the software and their comparison with what was theoretically expected.	27
Figure 4.10. Dynamixel® 2XL430-W250-T [24].	28
Figure 4.11. Dynamixel® XM430-W350-T [25].	29
Figure 4.12. Dynamixel® XL430-W250-T [26].	29
Figure 5.1. Load path computed by the software for the “Middle Link”.....	32
Figure 5.2. Representation of the manual adjustment process for the “Middle Link”.	32
Figure 5.3. Comparison between the “Middle Link” before and after optimization.	32
Figure 5.4. Load path given by the software for the “End link”.	33
Figure 5.5. Illustration of the adjustment process for the “End Link”.....	33
Figure 5.6. Comparison between the before and after optimization for the “End Link”.....	33

Figure 6.1. Manipulator after the assembly process..... 36

Figure 6.2. Glimpse of the developed gripper. 37

Figure 6.3. Overall perspective of the robot. 37

Figure 7.1. Differences between accuracy and repeatability. 39

Figure 7.2. Setup for repeatability measurement. (a) X axis; (b) Y axis; (c) Z axis. 40

Figure 7.3. The robot handling a 400 g load..... 40

Figure 7.4. Myo™, a gesture control armband developed by Thalmic Labs™..... 40

Figure 7.5. The five Myo™ built in gestures (a), which can be combined with each one of the following postures of the forearm: (b) Up; (c) Extended; (d) Down. 41

Figure 7.6. Confusion matrix of the Myo™ armband for: (a) Regular user; (b) New user A; (c) New user B. Each gesture was performed 20 times. 42

LIST OF TABLES

Table 2.1. Main differences between industrial and lightweight robots (adapted from [2]).	6
Table 2.2. Comparative performance analysis of some lightweight robots (adapted from [2]).	8
Table 3.1. Predicted movement range for each joint of the manipulator.	16
Table 4.1. Predicted maximum torque for each joint (in Nmm).	27
Table 4.2. Some of the main characteristics of the selected actuators.	29
Table 5.1. Overall improvements with the application of topology optimization.	34
Table 6.1. Printing parameters.	36
Table 7.1. Matching table for the final assessment, using the mentioned interface.	41

LIST OF SYMBOLS AND ACRONYMS

List of Symbols

θ – Angle between the direction of the force and the line towards the pivot point

τ – Torque

d – Distance from the point where force is acting to the pivot

F – Magnitude of the force

g – Gravitational acceleration

m – Mass

W – Weight

Acronyms

3D – Three-dimensional

AM – Additive Manufacturing

BLDC – Brushless Direct Current

CAD – Computer-Aided Design

DFKI – German Research Center for Artificial Intelligence

DLR – Institute of Robotics and Mechatronics of the German Aerospace Center

DOF – Degrees of freedom

EMG – Electromyography

FEA – Finite Element Analysis

FPGA – Field Programmable Gate Array

HRI – Human-Robot-Interaction

IMU – Inertial Measurement Unit

PET-G – Polyethylene Terephthalate Glycol

PLA – Polylactic Acid

STL – Stereolithographic format

TO – Topology Optimization

1. INTRODUCTION

The idea of having machines that can replace humans in different tasks has been around for centuries. However, in the last decades, with the appearance of robots, it has gained a whole new dimension.

A robot is commonly described as a machine that can perform a complicated series of tasks by itself. In fact, if we look closer, more than ever we are surrounded by them, as they are no longer just the machines, we used to see in industrial environments doing repetitive jobs. Nowadays, they can adopt numerous configurations according to their function, and perform such a diversity of activities from vacuuming the floor to ultra-precise surgeries [1].

In this case, this work will be especially focused on the lightweight robotics field. These robots, which usually assume the shape of a robotic arm, are carefully designed to prioritize mobility and the possibility of interacting in unknown environments, or even with humans. This last aspect has been, indeed, a major topic of research in recent years, given the enormous advantages the close collaboration between robots and humans will bring [2].

1.1. Problem and motivation

In recent years, lightweight robots have become increasingly common. However, the majority of solutions available on the market are still full-sized robots, usually conceived as high-end products. For that reason, those machines turn to be quite expensive, as they generally demand technically advanced solutions, materials, and research.

In order to explore that issue, this work aims to design and prototyping a low-cost compact lightweight robot manipulator, with six degrees of freedom (DOF), capable of high repeatability, accuracy, and maneuverability. Besides that, the overall target is to create a compliant robot, that can safely operate in close collaboration with humans. To achieve that, throughout conception, there will be a concern about optimizing the overall weight, while developing a structural design that is not only capable of reducing vibrations during motion but also allows complete integration of the compliant motors or mechanical transmissions (if needed). At the end of this project, it is expected to have developed a fully

functional robot with an overall satisfying performance, which will be used as a platform for future research and experiments.

As may be expected, this will be a multidisciplinary engineering project, combining areas such as mechanical design, mechatronics, automation, control, and programming, among others. Despite that, the present work will be primarily focused on the structural design, trying to achieve the desired performance by optimizing the components, while maintaining simplicity and maximizing characteristics such as high payload and low weight.

1.2. Proposed approach

Since this type of robot may interact with humans during operation, the design becomes a key point in their development process. For safety reasons, reduced mass and inertia are extremely desired so, typically, two approaches can be taken: use of lightweight materials or optimization of structural components. In this case, the choice went through applying some optimization techniques.

The proposed approach consists essentially of two major parts. In the first one, once the main desired guidelines for the manipulator are established, it will concern the design and optimization of the structural components needed, as well as the selection of the actuators. On the other hand, the second part will regard the manufacturing process, assembly, and some experiments to evaluate the final performance of the robot.

One of the major efforts in this work will be the integrability of all components. The cable management will be considered, and all actuators must be fully incorporated into the structure. In this last case, the aim is to carefully select them according to the structural design and torque needed in each joint, to which Dynamic Simulation from Autodesk® Inventor Professional 2021® is going to be used as guidance. Later, to keep the sprung masses as low as possible, the design of the links will be optimized by applying topology optimization tools from Autodesk® Fusion 360®.

Finally, from a manufacturing perspective, 3D printing will be used. This form of additive manufacturing was seen not only as a way of having more design freedom but also as a manner of keeping the cost low and, simultaneously, reducing the production time.

1.3. Thesis overview

This dissertation is composed of eight chapters, starting with the introduction of the subject and the formulation of the main objectives this project seeks to achieve. The second chapter surveys the state of the art on lightweight robots, with some of the current solutions available. The following one is used to establish the main characteristics that the prototype must have, while the fourth is dedicated to the first concept and its structural design. Then, the optimization of some components using topology optimization will be presented. The sixth chapter refers to the manufacture of the parts, as well as the assembly process, and it is followed by some experiments to evaluate the overall performance of the robot. Finally, the last chapter sums up the main results achieved and some future work to be done. Additionally, in the appendix, at the end of this work, there are technical drawings of the conceived components.

2. STATE OF THE ART

The original concept for the first lightweight robot results as an idea made manifest in 1991 by the Institute of Robotics and Mechatronics of the German Aerospace Center (*DLR*). Behind the main motivation of revolutionizing the robot applications in our society, the roots for the initial project also went back to the 1988-1993 ROTEX space program and the need for astronauts to have a similar robot on the ground that could handle gravity well (at that time standard robots were too heavy and not very powerful). The aim was to produce a machine inspired by the human arm with a load-to-weight ratio of 1:1 and identical performance. Since then, the *DLR* has created various prototypes first by itself and later in a partnership with the manufacturer KUKA[®], creating some of the most well-known solutions on the market [3], [4], [5].

The lightweight robots have been developed for application fields which are normally distinct from the ones covered by classical industrial robotics (Table 2.1). Typically, industrial robots are used in well-structured environments in which every operation is well defined and collisions with the environment or with humans can be a priori prevented. As they operate in dedicated work cells or caged areas, their strengths are mostly high position accuracy, high speed, robustness, durability, and relatively low price, being also the most suitable machines for performing recurrent tasks. However, these characteristics (especially the high positioning accuracy) demand high stiffness, which commonly results in a larger robot mass than its payload [6].

On the other hand, lightweight robots are carefully designed to operate in unstructured environments, where adaptability is required, and sometimes there is a need to operate in close collaboration with humans. For this reason, they must be light, while the ratio between self-mass and payload is kept low, not only to improve mobility but also to minimize injury risk in case of collision [2]. To prevent this last aspect, they should be capable of continuously monitoring their surroundings (searching for obstacles, for example), so a high number of sensors for sensing and control capabilities are essential.

Research in this field has increased significantly in recent years, mostly motivated by the versatility this type of robot can have and the ambition to achieve higher speed, less weight, and higher payload to weight ratio (while using smaller actuators).

However, it is important to note that, in these cases, there always be limitations in high absolute positioning accuracy, not only due to restricted accuracy on gathering information from the surrounding environment, but also as side-effects in design (e.g., large mass, and high stiffness) are definitely undesired. Intending to minimize these effects, recently, some studies [7] approached collaborative robot accuracy, aiming to explore redundancy in benefit of force capacity, as was proven that the force capacity of poly-articulated robots heavily depends on its articular configuration. The results looked promising, showing that with the described approach, the used robot would have force capabilities well beyond what is announced by its manufacturer.

Table 2.1. Main differences between industrial and lightweight robots (adapted from [2]).

Industrial Robots	Lightweight Robots
Fixed placement	Relocatable
Periodic recurring tasks	Common task changes
Rare interaction with the worker	Frequent interaction with the operator
Operator and robot separated by fences	Workspace shared with the worker
Profitable for medium to large lot sizes	Profitable even with small lot sizes

2.1. Design features of lightweight robots

It is the overall design and control capabilities that outstands these robots from others, whose mechanical design is mainly focused on reliable fulfilment of the tasks they are planned for. Once they are intended to operate in dynamic environments and possibly interact with humans, aside from the low mass, monitoring functionalities are crucial. Taking the *DLR* lightweight robots (Figure 2.1) as reference [6], it is evident that torque sensing and feedback are fundamental to increase not only the motion accuracy of the arm but also to monitoring and control the interaction forces. For example, during operation, position control must compensate the effects of robot elasticity, but even more important than that is the use of joint torque sensors. The combination between compliance and constant forces/torques measurement (in joints) is used to recognize collisions or contact with the surrounding environment and even, in some cases, a wrist force-torque sensor can be added for enhancing the precision at the robot end effector.



Figure 2.1. KUKA® LWR, the first commercialized version of the lightweight robot co-developed with *DLR*.

Another major advantage in these machines is the fact that joint torque sensors are usually placed close to the actuators, allowing passivity-based control methods [8]. This kind of approach enables the controller to precisely manage the amount of energy introduced into the system and opens the possibility of having predictive features, such as virtual inertias or multi-dimensional springs and dampers. Finally, there are other functionalities commonly adopted by these robots such as active vibration damping, sensitive collision detection, redundant position sensing, and Cartesian level.

After all, it must not be forgotten that the focus when designing a lightweight manipulator is generally to have a kinematic redundancy similar to the human arm. Picking up the *DLR* lightweight robot example again, the target was to build a high-performance seven degrees of freedom arm, with a load-to-weight ratio of approximately 1:1, a total system mass below 15 kg, and a range workspace up to 1,5 meters. Apart from these, as may be expected, the modularity and integrability of all components (either mechanical or electrical) were also key factors to achieve the desired system dynamics, so neither bulky wiring nor electronics cabinet were desired. In the end, the result was a 14 kg manipulator, capable of handling 15 kg at low velocity and with power consumption in normal operation sitting below 150 W (which is much lower than an industrial arm, for safety reasons also). In Table 2.2, there is a brief comparison with some of its closest competitors.

Table 2.2. Comparative performance analysis of some lightweight robots (adapted from [2]).

	Barret arm	DLR- KUKA lightweight arm	Mitsubishi PA10	Yaskawa- Motoman SIA5F
Number of axes - DoFs	4 or 7	7	6 or 7	7
Maximal payload [kg]	4	14	10	5
Repeatability [mm]	1	0,5	+/- 0,1	+/- 0,6
Working space [mm]	1000	935	950	559
Weight [kg]	25	14	40	30
Minimum installed power [kW]	0,06	0,150	1,5	1,0
Velocity [m/s]	3	2	1,55	/

As may be noticed from the previous table, lightweight robots are operated at relatively low velocity (especially compared to industrial ones), which typically demands higher gear ratios. In fact, HRI (Human-Robot-Interaction) robotic devices are still heavily conditioned by their gearboxes [9], as most of the time two unusual transmission technologies are required: Harmonic Drives[®] or Cycloid Drives. The *DLR* robots are no exception, as Harmonic Drive[®] gears and RoboDrive[®] motors were specifically developed to meet the desired requirements while focusing on high energy density, minimal power loss, and lightness. Besides that, the integrability of the complete drive train (motor, gearbox, sensors, and some electronics) in a single unit enabled its placement directly in the robotic joints, allowing better compliance and additional smoothness during operation.

However, all these advantages come at a price. Starting with the construction components, they must be lightweight (for maximizing the payload), so is common to have parts made from carbon fiber and other special materials, which tend to raise the robot price. In the same perspective, the need to minimize all components while meeting the aimed performance also contributes to making these robots less affordable. Additionally, in the design field, there are also some construction limitations. For example, it is common to have a central opening through the whole arm for dealing with the cable and pipe management, which raises the complexity of the parts (Figure 2.2). Finally, with the demanded increase in joint flexibility, less accuracy, and more complex system dynamics should be expected.

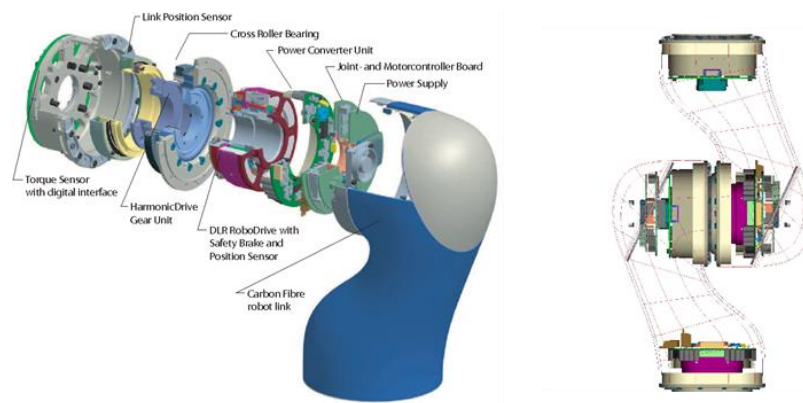


Figure 2.2. The mechatronic joint design of the DLR-KUKA® LWR [6].

While searching for other references more relatable to what is expected from the current project, another interesting one has shown up [10]. It is called *COMPI*, and it was developed by *DFKI*, the German Research Center for Artificial Intelligence. The *COMPI* (Figure 2.3) is a compliant robotic arm composed of six rotational joints, which is used as a research platform for dynamic control approaches. As being relatively compact, some of its characteristics stands out, for example, its tubular structural design, the use of external springs for helping achieve a payload of around 2 kg, or its overall mass of about 4,75 kg. To accomplish such performance, it uses *BLDC* (Brushless Direct Current) drivers with Harmonic Drive® transmissions and joint position sensors for absolute and incremental situations. Regarding some control features, once each actuator is controlled by one *FPGA* (Field Programmable Gate Array), it allows aspects such as position, velocity, and motor current management, as well as adjustments during runtime, or integrated friction identification and its compensation. In addition, a torque-based higher controller was also adopted to help handle the compensation of non-linear effects such as gravity and friction, but also to support the compliant control of the arm.



Figure 2.3. *COMPI* robot from the *DFKI* [10].

Lastly, other helpful projects that described how some low-budget robots were conceived or the employment of 3D printing during their manufacturing had brought up. For example, in [11], the first 3D printed prototype of a future lightweight manipulator intended to assist people with disabilities was presented. In [12], another case has portrayed the development of a 4DOF low-cost robotic arm, while in [13] a 3D printed robot was suggested for educational purposes. Additionally, in [14] and [15], similar approaches have gone even further, with the application of artificial intelligence elements and force limiting features, respectively.

2.2. Safety approach

Naturally, it is impossible to talk about applications featuring HRI devices, without questioning their safety for both, humans, and machines. In fact, the safety of collaborative robots has been an active research subject in recent years [16], [17], [18].

In that direction, also several health and safety regulations for industrial collaborative robots have been established in Europe, being two of the most relevant the ISO10218-1 [19] and ISO 10218-2 [20]. These led to the classification of cobots in four major groups, according to their safety, programming features, or even the strategy they use to avoid potential collisions with humans:

- **Power and Force Limiting:** collaborative robots which are built adopting rounded corners, combined with a range of intelligent collision sensors to quickly detect any contact, and stop the operation if needed. These robots also feature force limitation to ensure low injury risk;
- **Safety Monitored Stop:** cobots for applications that have minimal interaction between the robot and operators;
- **Speed and Separation:** usually, they pack more advanced vision systems, that allow to gradually slow down operation as worker approaches, and stop it only if the system detects operator is too close;
- **Hand Guiding:** in this case, motion can be directly controlled using a hand-guided device (which can be extremely helpful for manipulating heavy workpieces, for example). Furthermore, it also brings the possibility to use similar features for programming the robot.

To highlight that these regulations contemplate every single robot designed for any degree of human interaction, as, even those which are not created for permanent collaboration, have to be equipped with safety capabilities to prevent any major accidents.

As a result, this project aims to achieve a robotic arm that has the essential requirements to fit the first category (Power and Force Limiting), so it can operate safely close to the operator.

2.3. Topology optimization

To keep the sprung masses as low as possible the approach chosen went by applying some optimization techniques. Topology optimization (TO) is a method that employs mathematical tools to improve material distribution in a part to be designed (Figure 2.4). In practice, it takes a specified 3D design space and optimizes the material layout according to a given set of loads, boundary conditions, and constraints. By doing so, it tries to generate a more efficient design that, sometimes, seems even inspired by organic shapes (once this technique does not have any predefined configurations). In the end, the result tends to be a more complex and lightweight design without compromising the structural strength of the part.

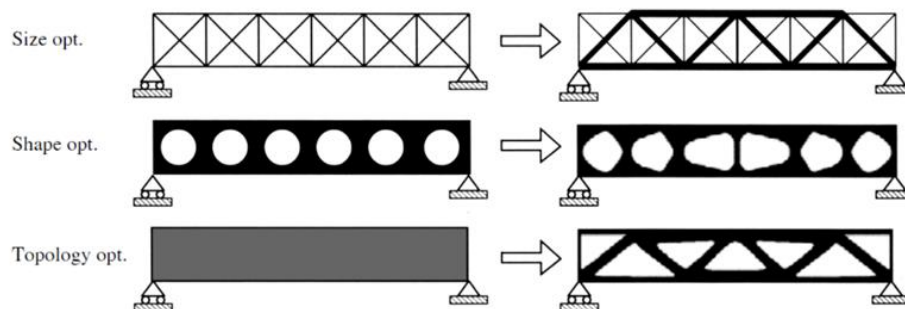


Figure 2.4. Comparative illustration of size, shape, and topology optimization [21].

Nowadays, this technology is built-in in a variety of CAD software and has a wide range of applications. In the case of engineering, it is mostly used at a concept level of the design process because it allows exploring new solutions, as well as the ability to cut excess weight when needed. In general, topology optimization takes advantage of resources like Computer-Aided Design (CAD), Finite Element Analysis (FEA), and other optimization algorithms, to present the best solution within the design space. The procedure (Figure 2.5) normally starts with a rough initial CAD model, which is then analysed through FEA not

only to evaluate the distribution of stresses and displacements throughout the given design but also to display which areas are working efficiently. At this point, optimization can start by applying the algorithm that better suits the problem requirements and remove the areas which are not supporting significant applied loads or do not play any major key role in the performance of the part. After this iterative process, the result is usually a more organic shape that meets the objectives and constraints set for the design. However, normally, before sent it for production, it is still necessary to perform some CAD adjustments (turning the design smoother and more manufacturable, for example), as well as go through another validation using FEA tools to guarantee that requirements and performance are satisfied (Figure 2.6). It should be noted that the final solution is a direct result of the given problem formulation, so that step is crucial to achieving the best optimization possible.

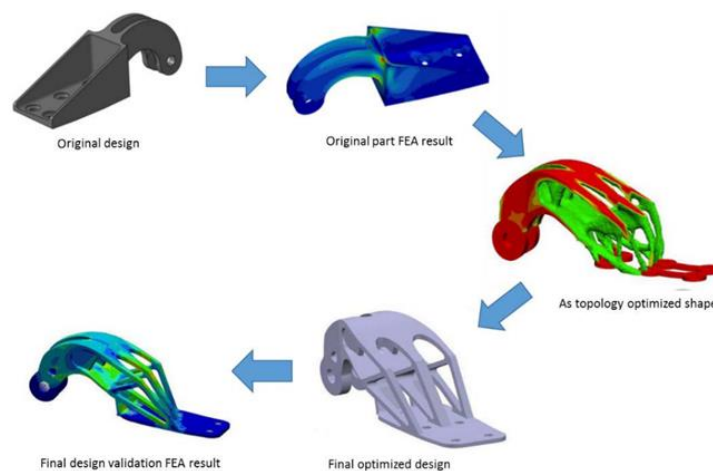


Figure 2.5. Usual steps of topology optimization process [21].

After all, as it is easily understandable, structural optimization can have a huge impact on the development process of a product. Among other benefits commonly associated, some stands out, such as the possibility of creating lightweight structures, the reduction on time-to-market, material savings, and the fact that it tends to reduce the amount of processing energy used, as well as the need for physical tests and prototype builds [21].

On the other hand, this technique has also been extremely benefited, recently, with the emerging of Additive Manufacturing (AM). Given the complex geometries that usually outcomes from this procedure, production through subtractive manufacturing processes was often very difficult or even impossible. With AM that problem was solved as it provides more design freedom and the ability to create almost any shape, due to its layer-

by-layer construction. Besides that, it usually reduces the production cost and time, while still delivering good precision regardless of the size of the part. Even though there are several technologies available based on this additive concept (covering a wide range of materials from metal to plastic), 3D printing may be the most common and well-known one.

Moving forward with some real application examples, in [21] the employment of this method has resulted in a 65% weight reduction of a jet engine bracket while meeting all its original requirements. As another illustration, a 4,7% weight reduction was achieved during the improvement of the pelvis module from the humanoid robot “*Sweaty*”, the runner-up world champion of the 2018 RoboCup [22]. Nonetheless, it is important to highlight that fields of application of topology optimization are almost endless, as have been shown in [23], where authors evaluated its use during the development of a 3D printed mandibular bone implant.

To sum up, topology optimization is a powerful tool that allows the accomplishment of lightweight designs, that can bring huge benefits, such as, saving time, material, and energy. It improves the overall design characteristics of a new or already existing product while maintaining its functional requirements, however, this technology is a bit useless if, in the end, the final design cannot be produced. So, what makes it interesting is the combination with additive manufacturing (for example), which allows taking a completely different approach to the designing process with fewer restrictions on how it will get produced or assembled.

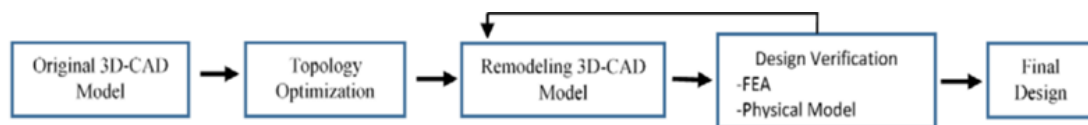


Figure 2.6. Typical design process while using topology optimization [21].

3. LIGHTWEIGHT ROBOT CONCEPT

As mentioned before, one of the main objectives was to conceive a compliant robot that was short, robust, and light. To accomplish that, the actuators should be carefully selected to deliver the features needed, while the structural links between joints should be cautiously designed to maximize the performance of the robot. It was precisely in this last aspect where most improvements could be made, therefrom the ambition to apply topological optimization for reducing the global structural weight and that way enhancing the payload capacity. Thereby, the links design was divided into two major parts: the first where a geometry that met the functional requirements had been established, and then, a second one, where those components were optimized.

3.1. Desirable characteristics

Despite it was settled, from the beginning, that the final result should be compact, it did not mean that the overall performance of the manipulator should be compromised.

It was established that the manipulator should have a maximum reach between 400 and 500 mm. That was considered a good compromise, once a bigger reach would probably imply not only hefty actuators but also a more robust structural design (bringing disadvantages in both, weight and compacity) and less than that would possibly turn the robot a bit useless.

On the other hand, it was delineated that ideally, the robot should be capable of handling a payload of around 400 g. This value was perceived as a plausible amount, having in consideration the mass of the tool (which can be changed accordingly to the task to execute) and the load itself, being also in line with the average for a manipulator this size.

Another subject that was evaluated was the expected movement range for the manipulator, which was translated as identifying the angular freedom each joint should have. Inevitably, that approach was only a conjecture, since, during conception, more design constraints were awaited. Thereby, at that point, it was considered sensible the following movement range (Table 3.1).

Table 3.1. Predicted movement range for each joint of the manipulator.

Identification	Angular range (in degrees)
Joint 1	360°
Joint 2	180°
Joint 3	180°
Joint 4	180°
Joint 5	180°
Joint 6	180°

3.2. Design and drafting

The structural design would always be closely related to the actuators that were chosen, once their size, geometry, or way of attachment would be different according to model and manufacturer. So, from the beginning, it was evident that the selection of the actuators would be an iterative process since without adopting one as a reference, it was not possible to make a first draft of the robot.

To help deal with the previous issue, the idea was to estimate the maximum required torque in each joint and use it as guidance for the selection of the motors. However, at that stage, it was not possible to do an accurate analysis, as structural weight and dimensions were unknown (that study would take place further in the project), but it was conceivable to make a rough evaluation to at least not oversize too much the actuators picked as the first reference.

From observing other robotic arms available on the market, it was verified that commonly they are composed of three or four distinct structural links. In this project, a similar approach was desired, as it seemed to represent the best compromise for functionality. Thus, it was concluded that ideally there would be three links: two of them around 150 mm, and the third, which would be mainly for assuring the connection between the last joint and the tool, would be about 50 mm.

After the last suppositions, it was viable to perform a rough analysis to estimate the required torque in some sections of the robot, allowing that way to have a notion of its magnitude. That simplified analysis, which considers only the desired payload of 400 g and the length of the links, is then presented in Figure 3.1.

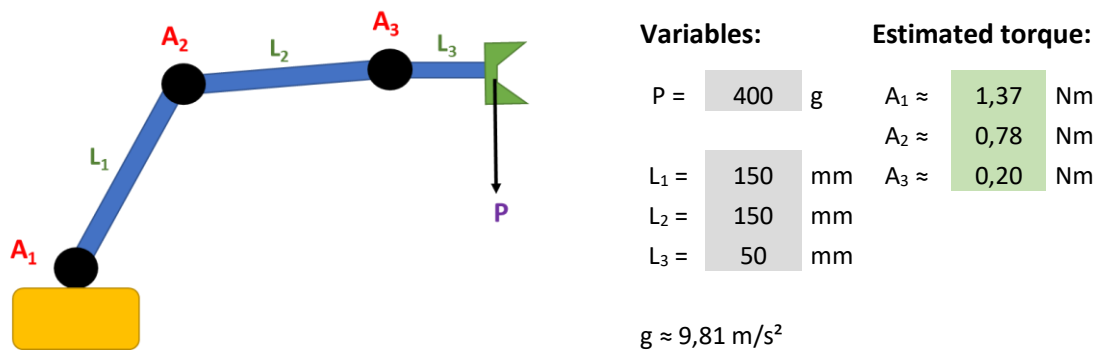


Figure 3.1. Rough analysis of the predicted torque by sections.

According to the results, as may be expected, the joint that is located at the bottom of the manipulator would be the one where more torque would be requested (with a value around 1,37 Nm). However, it is important to remember that neither gravity, nor actuators length, nor components masses were considered, so all the results would be clearly below what the real ones would be. In this regard, it was believed that applying a factor of 1,5 to the given values, would result in a more realistic approach. That way, it was expected that any actuator located at the bottom of the manipulator should provide around 2,1 Nm of torque, while the ones in the middle section of the robot should deliver about 1,2 Nm. Finally, it was concluded that the actuators near the robot end-effector, could be less powerful, with an estimated required torque around 0,3 Nm.

At this point, the first selection of the actuators was more feasible, as now there was a parameter that can be used as guidance. From there, after some research, one particular hypothesis seemed interesting: the possibility of using servos that are capable of handling two axes in a single unit. With this idea in mind, the model *2XL430-W250-T* from the manufacturer Dynamixel® came up, and since it was able to provide the predicted torque for upper sections of the manipulator, it was accepted as the first reference for them. However, for the lower area, once it was uncertain if there were any two-axis actuators capable of delivering around 2,1 Nm, it was decided that there still be considered the application of two separated modules.

4. STRUCTURAL DESIGN

With the assumptions made in the preceding chapter, it was possible to begin with the design iterative process. After several drafts, it was concluded that aside from the actuators, four main distinct structural components would be needed: a bottom part, two pieces intended to be used as a connection for the intermediate sections and, another one, to be placed at the robot end effector. With that concept in mind, it was finally achieved what was believed to be the best design compromise (Figure 4.1).

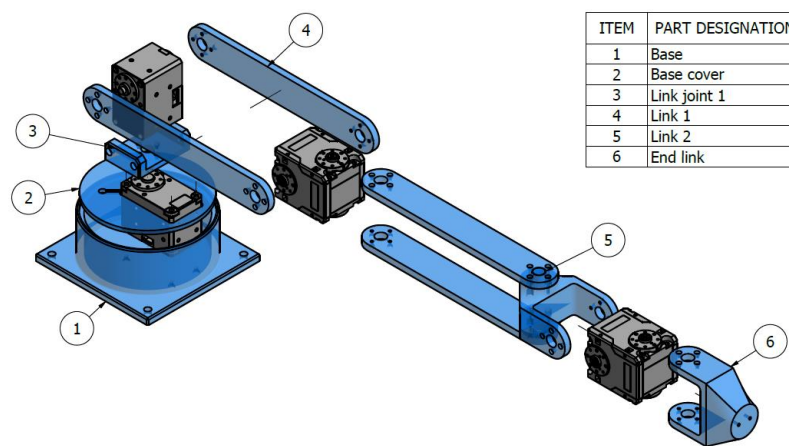


Figure 4.1. Outcome concept design for the manipulator.

As can be seen, the idealized concept was especially ruled by simplicity and functionality. At the same time, this approach already took advantage of using the two-axis actuators that were mentioned previously, while still considering the usage of two single-axis servos at the bottom for precaution. This is only the global perception for the parts, which are going to be described in more detail in the following section.

4.1. Parts geometry

Starting with the “Base” of the robot (Figure 4.1), the design freedom for that piece was quite plenty. Once its primary function was assured (ground the entire set), some different configurations and shapes could be adopted. That way, the overall idea was to conceive a simple part, where the bottom actuator could be attached and simultaneously would provide enough stability and rigidity to the entire structure.

On the other hand, the design of the links was one of the most challenging parts of this project. Despite not having any prior requirements (apart from their functionality), these components were crucial as they cannot compromise the overall structural integrity. In the same way, their weight would have a great impact in determining whether or not the manipulator met the desired capabilities (especially as they would be sprung masses).

Initially, as explained in the last chapter, it was decided to adopt a length of about 150 mm for each intermediate section of the manipulator and around 50 mm for the link that sits next to the end effector. After some drafts, it was concluded that the best solution for “Link 1” (Figure 4.1), would be using two separate pieces that would attach to each side of the actuators, instead of a single component. The idea was to draw a simple flat part, with its terminations matching the actuators mountings (where they would later be bolted). The outcome was a piece with a distance of 140 mm between actuators axes, 24 mm width, and 5 mm thickness, which was designated as “Middle link”.

In the same way, a similar idea was aimed for “Link 2” (Figure 4.1), however, it was realized that two consecutive joints have to be perpendicular to each other (otherwise, those DOF would be redundant). The solution came up with using three bolted components (two of the same “Middle link” as in “Link 1”, and an extra one denominated “Adaptor Joint 5”), since printing that geometry in a single part would be too problematic. The new part has a distance of 35 mm between axes, driving “Link 2” to a total length between joints of 175 mm.

Lastly, for the “End link” (Figure 4.1) a single part was desired, once it was planned that it would end on a circular section (allowing that way for any tool to be attached). Attending to that, the result achieved was a piece with 50 mm between the joint axis and the circular surface.

Additionally, two more pieces were conceived. First, the “Link Joint 1” (Figure 4.1), was intended to enable the connection between the bottom actuator (which promotes the rotation of the arm) and the following one. Secondly, the “Base cover” (Figure 4.1), which despite its mostly aesthetic function, will also help to manage the cables.

Although the geometry of the pieces presented in Figure 4.1 may appear to be the final one, it is important to remember that some parts would still undergo through the optimization process, so shape and dimensional adjustments must be expected.

Another aspect to highlight at that point was the necessity to define a material, so that way the software could compute the weight of the parts during torque analysis. That did not mean it could not be changed later, but the closer to the final material the better. So, since the plan was to use 3D printing, between many available options, the material assumed was PET-G (Polyethylene Terephthalate Glycol) with a specified density of 1,27 g/cm³. With that assumption, the expected mass for each “Middle link” piece was around 23 g (46 g for the set of two), about 30 g for the “Adaptor Joint 5”, 38 g for the “End link” and nearly 117 g for the “Base”.

4.2. Torque analysis

The selection of the actuators was an important part of the project, especially as it would have a great impact on the future performance of the robot. Despite the various approaches that could be taken, in this case, the ambition went by trying to predict the maximum required torque in each joint, so it could be used as guidance while choosing the actuators.

The mentioned analysis was performed using a tool called Dynamic Simulation from Autodesk[®] Inventor Professional 2021[®], which allows modelling the behaviour of a dynamic system throughout the time while delivering some data about the parameters that are involved (e.g., forces, moments, velocities, accelerations, etc.). This tool was chosen as it is straight implemented in CAD software (making it easier for switching between construction and simulation environments), but also as it allows great adjustability of the input parameters. Nevertheless, despite Dynamic Simulation provides the results within seconds, their understanding and validation are still crucial to ensure they match the intended situation.

For this approach, as mentioned before, the variable that had a particular interest was the moment (or torque) in each joint, which, in physics, is the rotational equivalent of a linear force. Typically, the moment is represented by the Greek letter τ and is given by the following equation:

$$\tau = F * d. \tag{4.1}$$

However, as forces (during the rotational movement), do not always act perpendicular to the line that joins the point of application to the pivot point (Figure 4.2),

most of the time is necessary to do a small transformation using sine (or cosine, depending on the situation) as exemplified under:

$$\tau = F * d * \sin(\theta). \quad (4.2)$$

In this case, F is the magnitude of the force acting on the object, d is the distance from the point where force is acting to the pivot and θ will be the angle between the direction of the force and the line towards the pivot point.

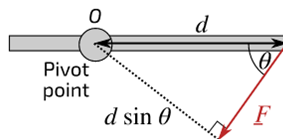


Figure 4.2. Illustration showing the perpendicular distance between the force (F) and the pivot point.

For a better understanding of the Dynamic Simulation environment, the idea was to start with the simulation of a basic assemble of two parts band together by a rotational joint (Figure 4.3).

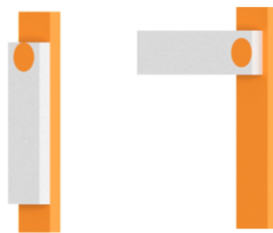


Figure 4.3. Illustration of the one-joint elementary assembly, showing 0 and 90-degree position.

The exercise consisted of a comparison between the results given for this situation by the software, and the ones estimated by adopting the previous formula, intending to see if they match. As may be expected, before starting, it was necessary to define some parameters such as parts dimensions, loads applied, and the range of movement in analysis. It was delineated that the test would be performed from a 0-degree position (both parts pointing down) to a 90-degree position (pieces perpendicular to each other), once values are periodic for 180 or even 360 degrees. It was also decided that would be applied a 4 N force (simulating a load about 400 g) on the end face of the moving part, which distances 100 mm from the pivot point. Finally, there would be considered two scenarios: with and without considering the influence of gravity. The second one, would not only act as a “control group”, but it would also help understand how Dynamic Simulation computes the

gravitational effect. The comparison between the software results and the theoretical ones, for the second situation, is presented in Figure 4.4.

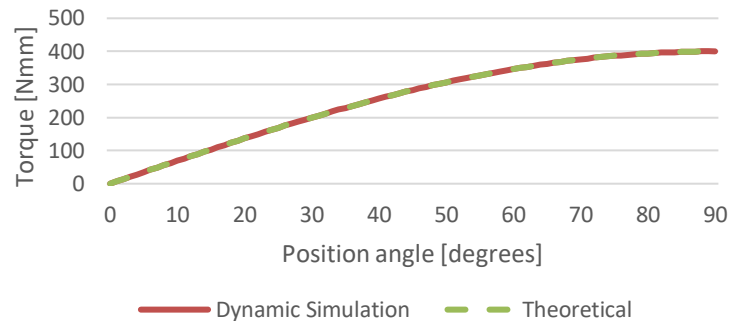


Figure 4.4. Results for the one-joint elementary assembly, without considering gravity effect.

As can be seen, by the graph above, there is a perfect match for this situation, which was a good indicator for the next steps. In this case, for example, the maximum torque of 400 Nmm is required when the parts are perpendicular, which was expected given the 4 N force and the 100 mm distance from application point to pivot.

With the previous situation verified, it was time to move on to the next step, where the biggest question was how Dynamic Simulation would compute the gravitational effect. To begin, the weight of an object is given by the following equation, where m is the object mass and g the gravitational acceleration (which was assumed as approximately 9,81 m/s^2):

$$W = m * g. \quad (4.3)$$

Without having a clue on how Dynamic Simulation would take the gravity influence and unsure of the approach to take, the starting point was to test the most obvious one: the software would consider the weight as a vertical force on the center of gravity of the object. For this, it was necessary to know the center of gravity of the part (which was proven to be given by the software), allowing that way the calculation of the distance from it to the pivot point. In Figure 4.5, there are the results for this situation.

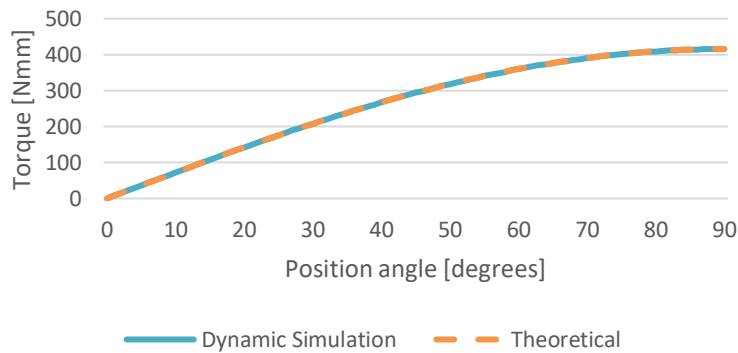


Figure 4.5. Analysis of the one-joint elementary assembly, considering gravity effect.

One more time, through the displayed graph, it seemed that the results given by Dynamic Simulation matched the theoretical ones calculated (some minor differences were identified, probably due to rounding in the value of gravitational acceleration). Despite that, it was still possible to conclude that the previous assumption was verified, this is, the software considers the gravitational effect as a force (weight) applied to the center of gravity of the part. This outcome in this simpler assemble was crucial for the next steps of the project, as it would allow to always have a rough guideline of what is expected in each situation (even though the data from the software will always be more precise).

Additionally, it was also tested a second configuration which has two joints instead of one (Figure 4.6). The objective of this assembly was to verify if the assumptions were still well-founded.

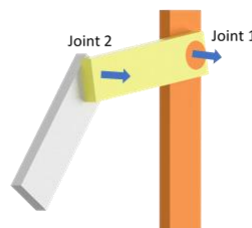


Figure 4.6. Illustration of the two-joint elementary assemble with indication of the first and second joints.

As can be seen, by the figure above, the overall idea was similar to the previous one, with one joint between the orange and yellow parts (Joint 1) and the other, between the grey and yellow pieces (Joint 2). Besides, there still be considered a 4 N force at the end face of the grey part (which now distances 190 mm from Joint 1 and keeps 100 mm from Joint 2), and the range of movement was kept from 0 to 90 degrees (being the 0 position when both parts are pointing down). Finally, the analysis still considers both situations: without and with gravitational effect (Figure 4.7).

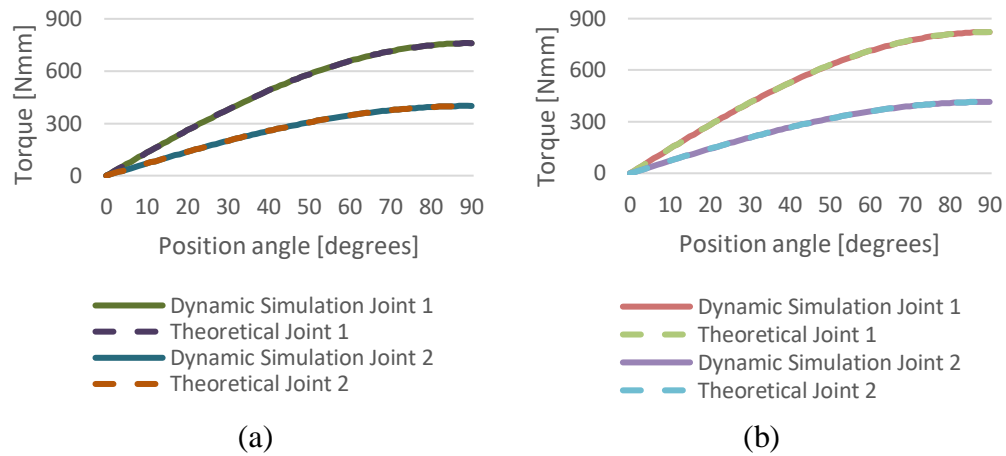


Figure 4.7. Analysis of the two-joint assemble without (a) and with (b) gravitational effect.

As may be noticed, in both cases and for the two joints, there is an excellent coherence between the values of torque given by the software and the ones that were theoretically expected. Therefore, it was viable to conclude that this approach was also valid for this configuration, so it was assumed that there should be no problem with future more complex assemblies. With that result, it was time to move forward and apply the same method to the full model.

Before starting, it was important to remember how the overall concept has been set up and understand where each joint was placed, for which, Figure 4.8 can be useful.

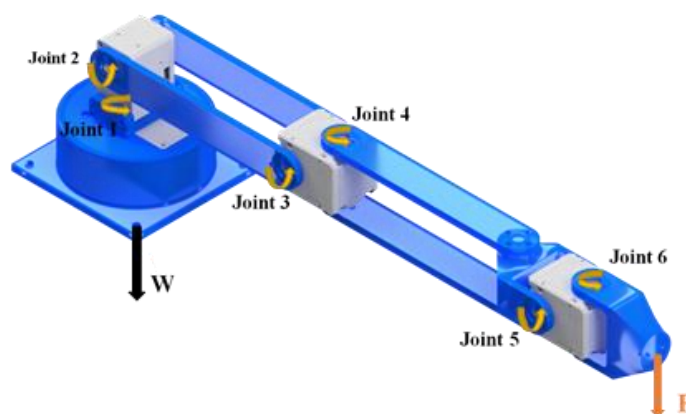


Figure 4.8. Identification of the joints, as well as the forces which will be considered in the analysis.

The idealized study will be quite straightforward, having in consideration only the parts weight (W) and the same additional load of 4 N (F) at the end effector of the manipulator (slightly above a 400 g payload).

Once that analysis was mainly for evaluating torque (and attending to how it is calculated), there were two particular parameters of interest in those components: mass and length. However, from the early steps, one particular detail about Joint 1 stood out.

The first joint is a singular case since it is placed in a position to which every vertical force considered would have the same direction as its axis of rotation (attending that the base of the robot will always be fixed upright). That way, it is more difficult to evaluate the torque required, as, theoretically, the demanded moment will not result from the structural weight itself, but from the global moment of inertia combined with the acceleration of the arm. Since those specifications were uncertain, the strategy went through oversizing and accepting a maximum predicted torque of 1,5 Nm for that joint, as it was considered reasonable.

Proceeding with the remaining joints, the approach was more similar to what was seen in the first place. The strategy was always trying to take the least favourable position for every joint and then perform the analysis while varying the angle of rotation from 0 to a 90-degree position with a step of one degree at a time. At this point, it was also important to highlight that the only actuators which must be contemplated, are the ones from Joint 3 to 6 since the remaining can be considered unsprung masses. So, considering the preference to adopt the two-axis actuators in those joints (around 98 g of mass each), they will be the only ones which selection has a direct repercussion on the torque values obtained.

Finally, after the last assumptions, the results from the software could be gathered. Figure 4.9 shows up those results and their comparison to what was expected. In addition, Table 4.1 displays the maximum torque value attained for each joint.

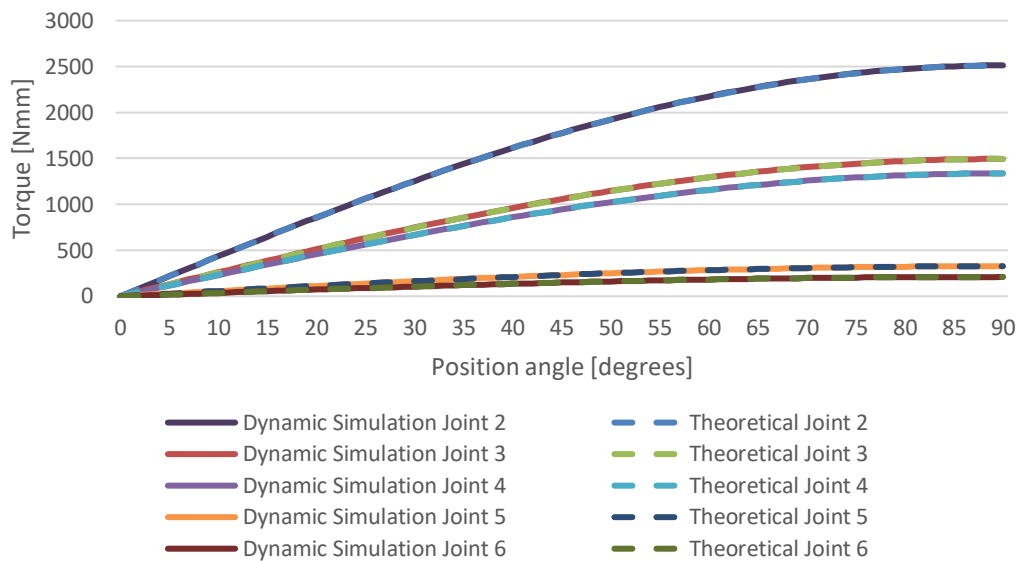


Figure 4.9. Results given by the software and their comparison with what was theoretically expected.

Table 4.1. Predicted maximum torque for each joint (in Nmm).

	Joint 1	Joint 2	Joint 3	Joint 4	Joint 5	Joint 6
Maximum required torque [Nmm]	1500	2512,74	1494,37	1336,82	327,07	210,52

After this analysis, it was possible to conclude that, as was expected, the maximum torque requested would take place on Joint 2, with a value around 2,5 Nm. From there, the amount needed would decrease as the robot end-effector gets closer. To highlight that those values would probably not be the final ones since structural optimization was not done yet.

4.3. Selection of the actuators

After the previous analysis using the earlier selected actuators, it was possible to take some conclusions. As seen in the last section, the maximum required torque was located on Joint 2 with a value around 2,5 Nm, while for the remaining cases, the predicted torque would sit below 1,5 Nm. However, it is important to remember that those are only indicative figures, as regarding safety, is always better if the actuators could exceed those values by a considerable margin.

One particular requirement that was placed, at that point, was the input voltage for the actuators, which, given the power supply units available, was established as being of 12 V. Although it can be a bit underestimated, this parameter is crucial, since it has a direct impact on how much torque the servos will be capable of delivering.

On the other hand, it was recognized that, ideally, the servos should aggregate all the components and features needed in a single unit. Between those, compliance was seen as a must, especially to guarantee the aimed level of safety during operation. A compliant actuator, usually allows small deviations from its equilibrium position (commonly characterized as being the position where the actuator delivers zero force or torque), enabling that way to have better control feedback and less rigidity in case of collision.

Moving forward with the selection for the upper sections of the manipulator (elbow and wrist), the ideal scenario was if the previously suggested model could meet the desired requirements. According to the manufacture Dynamixel[®], the *2XL430-W250-T* (Figure 4.10) is described as a fully integrated smart servo module, capable of delivering up to 1,5 Nm (at 12 V) and with the particularity of allowing to control two axes with a single module. After a careful evaluation of its specifications, it was concluded that it suited the project requirements, so two of them would be adopted.



Figure 4.10. Dynamixel[®] 2XL430-W250-T [24].

With the previous actuator selected, there were more limitations to consider, being the most important one to ensure that all the servos were compatible with each other. That way, to avoid any undesired situations, it was settled that all the actuators would come from the Dynamixel[®] *X* family.

Proceeding with the Joint 2, it was soon realized that none of the two-axis modules available were capable of delivering the desired torque, as well as neither servos of the *XL* (Low cost) category. This situation led to the necessity of moving further in the product range to a Mid-Level Performance class (*XM*). The model chosen was the *XM430-W350-T* (Figure 4.11), which, as the previous one, was described as a smart actuator integrating the DC motor, controller, driver, sensor, and reduction gear in a single unit.

Besides that, this module is capable of delivering up to 4,1 Nm at 12 V, which is clearly above what was required. However, as it is only a single-axis actuator, it was still necessary to add a second module at the base of the robot to promote its rotation.



Figure 4.11. Dynamixel® XM430-W350-T [25].

Finally, for the shoulder of the robot (Joint 1), as there was no special requirement for a powerful unit, the choice went back to the *XL* category, more specifically to the model *XL430-W250-T* (Figure 4.12). Generically, this is the single-axis version of the first two actuators selected, so its characteristics are similar to the previous ones. Furthermore, it advertises a maximum torque of 1,5 Nm at 12 V, which is in line with what was expected.



Figure 4.12. Dynamixel® XL430-W250-T [26].

Once all the required actuators were selected, and to end this section, it is then presented a small table (Table 4.2), which sums up their most relevant characteristics for a 12 V input.

Table 4.2. Some of the main characteristics of the selected actuators.

Model	Stall torque [Nm]	No load speed [rev/min]	Current [A]	Gear ratio	Weight [g]	Dimensions (WxHxD) [mm]
2XL430-W250-T	1,5	61	1,4	257,4:1	98,2	36x46,5x36
XM430-W350-T	4,1	46	2,3	353,5:1	82	28,5x46,5x34
XL430-W250-T	1,5	61	1,4	258,5:1	57,2	28,5x46,5x34

5. STRUCTURAL OPTIMIZATION

Currently, there are several CAD software that offers built-in optimization tools, including topology optimization ones. In this project, the choice went through using Topology Optimization from Autodesk® Fusion 360®, as it revealed quite straightforward.

The aim of applying this technique was to, somehow, try to reduce the sprung masses of the manipulator, aiming that way to enhance its performance. Regarding that, it was established that “Middle link” and “End link” components would go through optimization, as they were seen as the parts with more potential for weight reduction.

To sum up, the procedure starts by having a fully defined part, which should have the desired material assigned. Then, all the constraints and forces applied must be specified, as well as regions that may be preserved and symmetry planes (if desired). Lastly, mesh parameters and shape optimization criteria must be established, in order to run the simulation.

Since there are some parameters that both parts will have in common, before stepping into the individual analysis of each piece, it was decided to define them. First of all, as may be expected, the gravity effect must be always considered. Secondly, it was thought that all the constraints or forces must be directly applied to the respective holes where the bolts will be placed, and those regions must be preserved to their original shape. Finally, it was outlined that each component must be capable of handling a 10 N force, which was already an oversized amount to guarantee additional safety. That way, it was ensured a safety factor above 2,5 for each part.

With the previous explanation in mind, the first part to be studied was the “Middle link”. The idea was to exploit its most favourable position, so it was settled that one end must be fixed while the other would have a vertical load of 10 N split by the four pockets. Later, a vertical symmetry plane was specified, as well as a tetrahedral mesh, which has an absolute size of 2 mm (resulting in 21188 elements and 5093 nodes). Having into consideration these parameters, in Figure 5.1 the load path computed by the software is displayed.

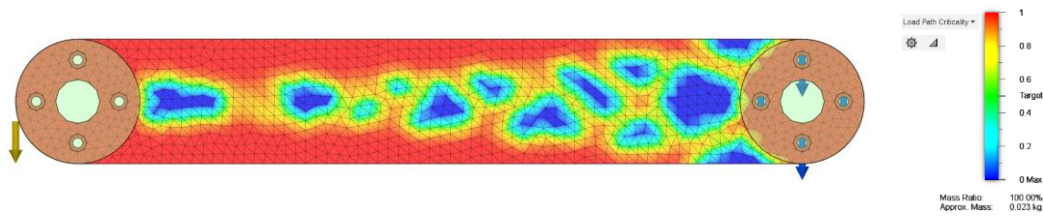


Figure 5.1. Load path computed by the software for the “Middle Link”.

After several experiments, it was concluded that, according to the simulations, the best achievable mass reduction without compromising the structural integrity was around 20%.

With that outcome, it was possible to start performing some adjustments to improve its aesthetics and the printing process (Figure 5.2). However, once those are made manually, it was precisely here that laid down one of the major limitations of the process, since, after all, there would be no single solution. Despite that, the whole effort was towards matching the geometry suggested by the software.

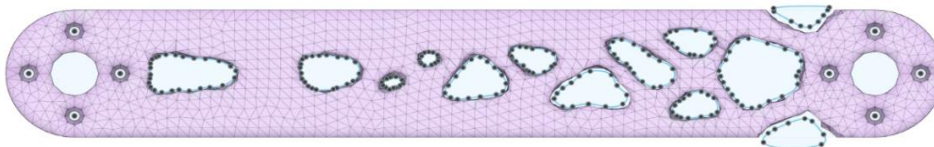


Figure 5.2. Representation of the manual adjustment process for the “Middle Link”.

Finally, for a better illustration of the progress made, a comparison between the initial and final design achieved is then presented (Figure 5.3).



Figure 5.3. Comparison between the “Middle Link” before and after optimization.

Moving forward, the optimization of the “End Link” was more challenging, mostly due to its geometry. A similar approach was taken (considering the eight small holes fixed and a 10 N force split by the two holes at the opposite end), however, at that time, it was realized that the mass reduction could be a little more ambitious with a target set around 30%. The mesh used was also tetrahedral, but the absolute size was set to 1 mm, which resulted in 194937 elements and 37442 nodes (Figure 5.4).

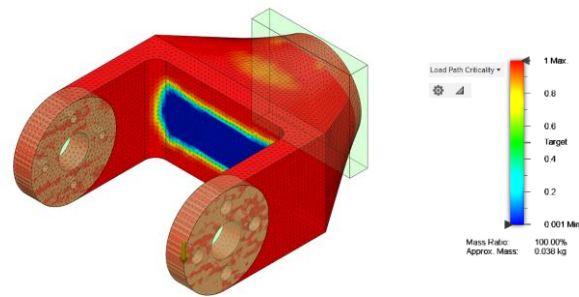


Figure 5.4. Load path given by the software for the “End link”.

In this case, as can be seen by the figure above, the suggestion was to create a crater from the inside face of the part. Once again, the post-processing and adjustments were manually made, so despite considering the geometry achieved a quite good approximation to what was suggested, it is not guaranteed that it perfectly matches (Figure 5.5).

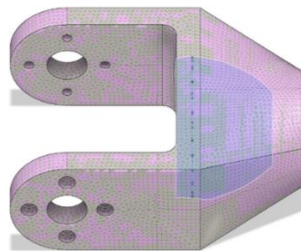


Figure 5.5. Illustration of the adjustment process for the “End Link”.

In Figure 5.6, the differences between the before and after optimization stages can be better perceived.

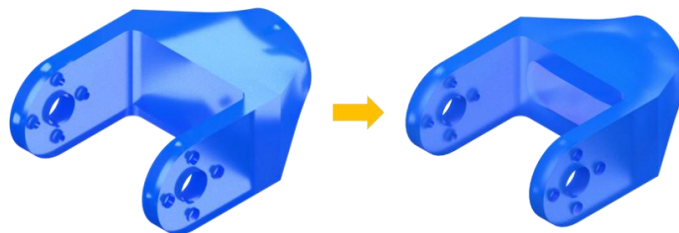


Figure 5.6. Comparison between the before and after optimization for the “End Link”.

Since the parts are relatively small and light, a large mass reduction was not expected, as otherwise their rigidity could be compromised. Despite that, the outcomes accomplished (presented in Table 5.1) were still considered quite interesting.

Table 5.1. Overall improvements with the application of topology optimization.

	Original mass [g]	Post-optimization mass [g]	Real measured value [g]
“Middle Link”	23	19	18,3
“End Link”	38	27	25,9

In conclusion, this process enabled a mass reduction of around 20% in the “Middle Link” piece and 30% on the end effector one. However, it is important to highlight that a conservative approach was taken due to expected uncertainties and limitations (small structural defects that could be introduced later by printing, for example). Even though the reduction may seem quite insignificant, it turns out to be an overall sprung mass reduction of around 27 g, which was seen as a good achievement for this work.

6. ROBOT MANUFACTURING

At that point, with all the actuators selected and the geometry of the parts established, it was time to start building the prototype. That way, the first step was to 3D print the pieces which were conceived. It is worth mentioning that all technical drawings of the designed parts, as well as the components list for the assembly process, can be found in the appendix at the end of this work.

6.1. 3D printing

The 3D printing process starts right after having a fully defined part, whose CAD file should be saved in stereolithographic (STL) format. This file, which only describes the geometrical surface of a 3D object, is later used by the slicer software (in this case Ultimaker[®] Cura[®] 4.8.0) to generate the horizontal layers with trajectories that the printer needs to manufacture the object. After this, the data must be saved in a g-code format file, so it can be directly used in the 3D printer, which, for this project, was BQ[®] Hephestos 2[®].

Regarding the material, there were two main options considered: PLA (Polylactic acid) or PET-G. Both PLA and PET-G are thermoplastics that belong to the polyesters group. They are two of the most commonly used plastics for 3D printing, and despite their similarities, there are some minor differences between them. Typically, PET-G has better physical properties and durability, while PLA is more used for parts that require good aesthetics. From a manufacturing perspective, PET-G also tends to be slightly trickier, demanding higher printing temperatures and bigger nozzle gaps.

After some discussion, and once the main concern for this project was not to compromise the structural integrity of the components, the choice went through using a 1,75 mm PET-G filament for every part manufactured.

6.1.1. Printing parameters

The input parameters given to the 3D printer, such as printing velocity and infill characteristics, are crucial to determine the final quality of the parts, so they must be carefully chosen. While assessing those decisions, one particular detail stood out: even though it seemed, after the first printing tests, that the links may not require 100% infill

density, it was clear that to have a good correlation to what was simulated previously, they must assume that value.

In a simplified way, the printing parameters which were used for each part are described in Table 6.1.

Table 6.1. Printing parameters.

	Base	Base cover	Link Joint 1	Middle link	Adaptor Joint 5	End link
Temperature	230 °C	230 °C	230 °C	230 °C	230 °C	230 °C
Nozzle size	0,4 mm	0,4 mm	0,4 mm	0,4 mm	0,4 mm	0,4 mm
Infill Pattern	Grid	Grid	Grid	Grid	Grid	Grid
Infill Density	35%	35%	100%	100%	100%	100%
Layer height	0,2 mm	0,1 mm	0,1 mm	0,1 mm	0,1 mm	0,1 mm
Print Speed	42 mm/s	35 mm/s	35 mm/s	35 mm/s	40 mm/s	35 mm/s
Adhesion type	Brim	Brim	Brim	Brim	Brim	Brim
Type of support	None	None	None	None	Everywher	None
Retraction	On	On	On	On	On	On
Heated bed	N/A	N/A	N/A	N/A	N/A	N/A

6.2. Assembly process

The assembly procedure itself was quite simple, as it mostly consisted of bolting all components together and connecting the indispensable cables. The accomplished result is then presented (Figure 6.1).

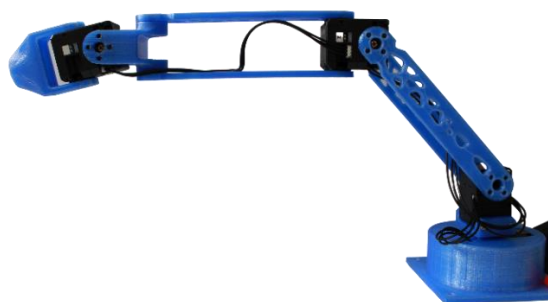


Figure 6.1. Manipulator after the assembly process.

Additionally, as a side project, it was developed a small gripper (Figure 6.2), as well as some parts to cover the middle section of the robot in order to enhance its aesthetics. In the first case, its overall concept was inspired by a project made in *TU Delft (Delft University of Technology)* [27]. The aim was to have a compact lightweight gripper that can be used in tiny robotic applications to pick up small objects. Therefore, since the gripper must suit the robot, it turned out relatively short with dimensions around 55 mm in length, 35 mm in width, and 42 mm in height. Besides, it uses an EMAX[®] ES08MAII servo and it has an overall weight of around 36 g.



Figure 6.2. Glimpse of the developed gripper.

Otherwise, since the shell components were mainly for turning the robot more appealing, their weight should be kept as low as possible once they cannot compromise its performance. The result was a design with 0,8 mm thickness and about 11 g each, which can be seen under, along with the overall view of the conceived prototype (Figure 6.3).

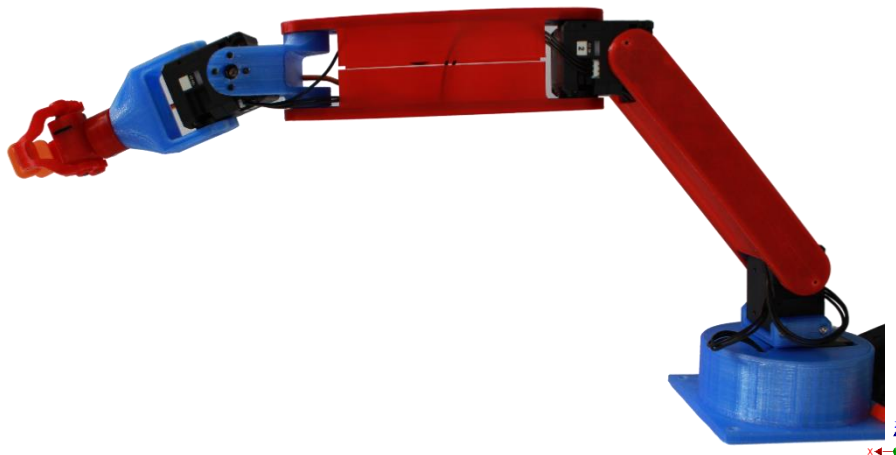


Figure 6.3. Overall perspective of the robot.

7. EXPERIMENTS AND RESULTS

As the manipulator was fully assembled, the next step was to evaluate some of its performance figures. Despite the several metrological characteristics that could be appraised to identify the effectiveness of the robot, it was outlined that the experiments would be particularly focused on two main criteria: precision and payload capacity. That way, in the following sections, the procedures taken will be described and other relevant features will be presented. To highlight that the gripper was not considered in any contemplated situation, since, after all, it is a changeable tool.

7.1. Precision

The precision of a device is, most of the time, seen as a subjective parameter once there is no direct method of measuring it. In fact, precision is frequently characterized by two other measurable attributes: accuracy and repeatability. In those, accuracy is usually defined as being the difference between the requested and obtained tasks, while repeatability can be described as the ability to accomplish repetition of the same task (Figure 7.1).

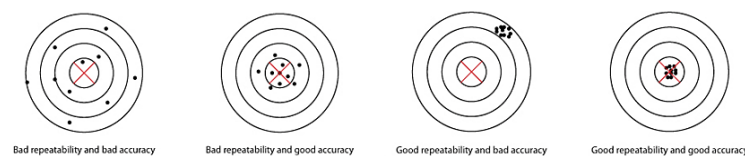


Figure 7.1. Differences between accuracy and repeatability.

Since there was not available a rigorous process for accuracy measurement, the realized experiments were limited to repeatability only. The procedure consisted of using a comparator placed on a stand (in a predefined position), so it could quantify the obtained deviation when a given trajectory was requested multiple times (Figure 7.2). Three directions (X, Y, and Z) have been considered, and each trajectory was set in a way that different joints should be used during the motion. The outcomes were quite pleasant, revealing values of 0,38 mm for the X-axis, 0,2 mm for the Y-axis, and 0,06 mm for the Z-axis. That way, it was concluded that global repeatability around 0,4 mm can be expected.

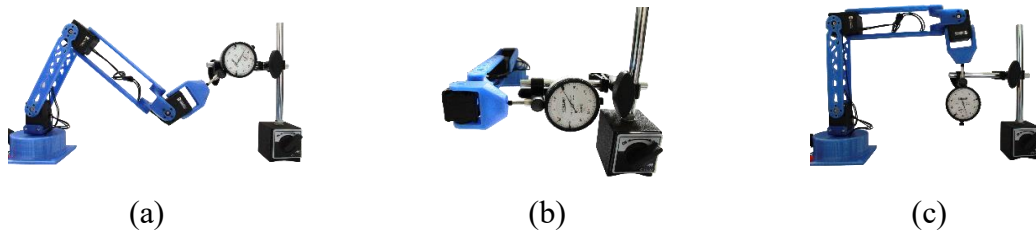


Figure 7.2. Setup for repeatability measurement. (a) X axis; (b) Y axis; (c) Z axis.

7.2. Payload

The adopted approach for the payload capacity was simple. It consisted of gradually increasing the load applied at the end effector, starting with a 100 g load.

In this field, the results were quite disappointing, with the actuators not delivering the expected performance. However, and despite those limitations, the handling of the desired mass (400 g) was still achieved (Figure 7.3).



Figure 7.3. The robot handling a 400 g load.

7.3. Control interface

Given the ambition that the manipulator should be able to operate in collaboration with humans, it was desired to ensure a reliable and intuitive interaction. In that regard, it was thought that implementing a gesture control interface could be a great advantage. There are already several works that have proposed gesture-based HRI approaches (e.g., [28]), however, in this case, it was intended a more simple, practical, and easy-to-use solution. That answer came up with the Myo™ armband (Figure 7.4) and was inspired by [29] (where one of those had been used for controlling a 6 DOF robotic arm).



Figure 7.4. Myo™, a gesture control armband developed by Thalmic Labs™.

The device is composed of eight EMG (Electromyography) sensors (which allow measuring the electrical activity of the forearm) and a nine-axis inertial measurement unit (IMU). Combined, they allow to recognize the motion of the arm and even to identify some hand gestures. In fact, by default, it has five built-in predefined gestures (Figure 7.5 (a)), that could be used to trigger different assigned actions.

For this project, the objectives consisted of developing an interface that could link the gesture recognition with the robot, as well as, somehow, widen the range of signs available. In the first case, the strategy used went through building a MATLAB® application, while employing *Myo SDK MATLAB MEX Wrapper* [30]. For the second, it was thoughted to combine the predefined gestures already available with forearm postures (Figure 7.5). That was made possible by using the acceleration vector given in real-time by the IMU.

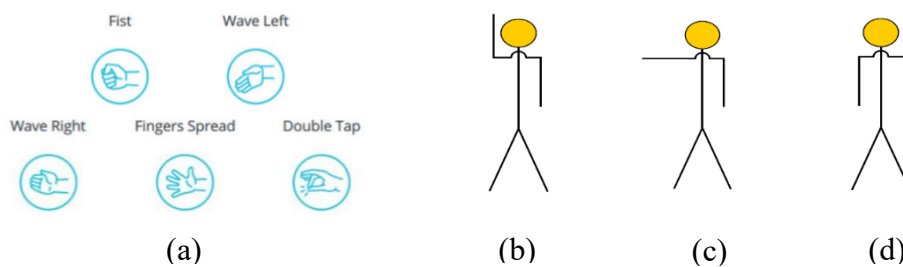


Figure 7.5. The five Myo™ built in gestures (a), which can be combined with each one of the following postures of the forearm: (b) Up; (c) Extended; (d) Down.

Later on, after the system was running and stable, a final assessment was made. It consisted of moving an object from a point to another by using the commands described in Table 7.1. The operation was performed without any issues and the responsiveness of the set was very pleasant, providing an intuitive and fluid experience.

Table 7.1. Matching table for the final assessment, using the mentioned interface.

Gesture	Posture of forearm	Operation
Fist	Up	Go to pick position
Fist	Extended	Close gripper
Wave left	Extended	Go to drop position
Wave right	Extended	Open gripper
Double tap	Down	Go to home position

In the end, the evaluation of this approach was quite positive, with Myo™ revealing truly handy and easy to use. Occasionally, there were still some minor issues with the misidentification of some gestures or postures, however, it was also concluded that those problems could be reduced with some setup adjustments. For example, the position of the armband in the forearm is relevant, as well as the distance to the Bluetooth® receiver. Additionally, the usage of a gesture custom profile for each user (instead of the default one) has proven to be helpful and some familiarization with the device is recommended for better accuracy (Figure 7.6).

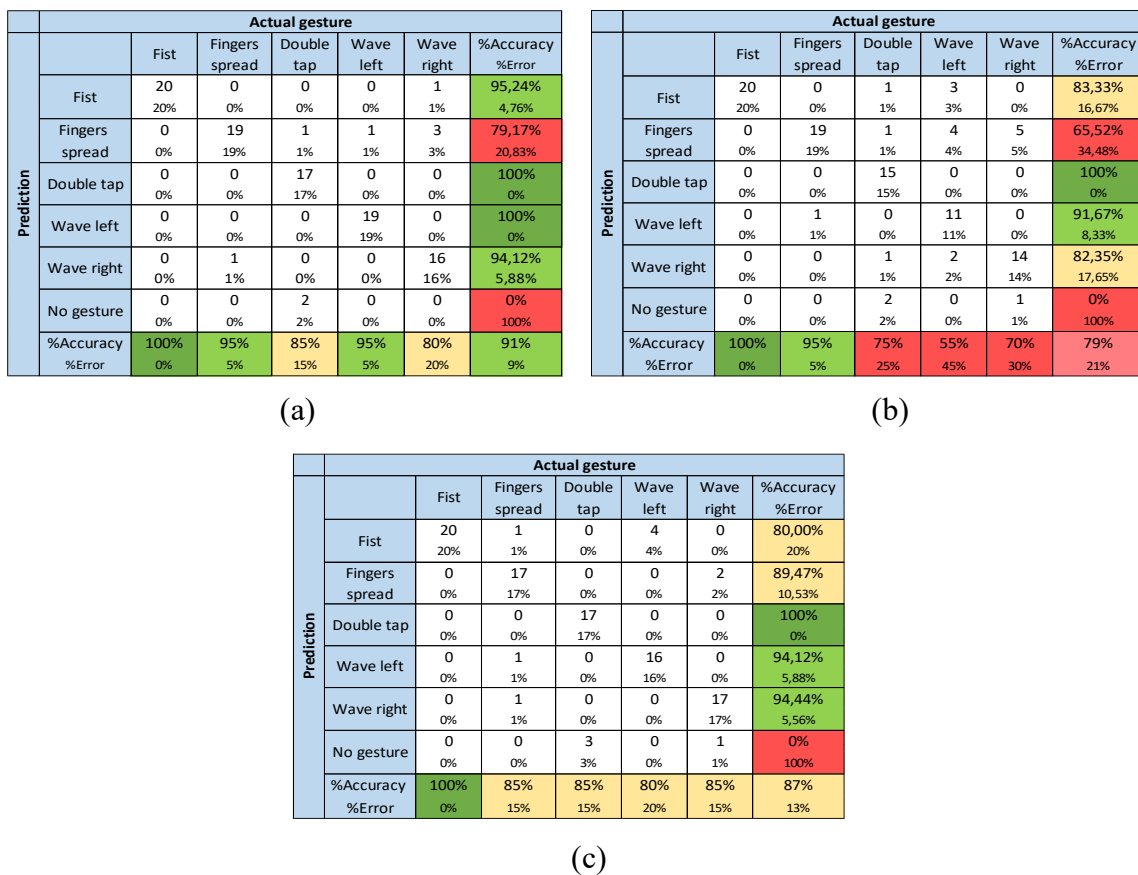


Figure 7.6. Confusion matrix of the Myo™ armband for: (a) Regular user; (b) New user A; (c) New user B. Each gesture was performed 20 times.

8. CONCLUSIONS

The present work describes the design process and manufacture of a small compliant lightweight robotic manipulator, with six degrees of freedom. The main ambition of this project was to create a fully functional prototype while applying some simulation and optimization tools to enhance its performance.

The final result revealed quite satisfying capabilities, despite it is still considered that a conservative approach in the designing process was adopted (especially to what topology optimization concerns). The finished robot provides global repeatability around 0,4 mm and it is capable of handling 400 g, which is believed to be quite remarkable attending its 678 g total mass. However, in this last field, the results fell short of expectations as some actuators could not deliver the expected torque specified by the manufacturer.

On the other hand, the overall set is able to deliver a smooth and nimble operation. Despite its small scale, the gripper can grab a wide range of objects without any problem. Regarding the gesture interface, it proved to be intuitive and effective. Besides that, it can be easily used by users with or without previous experience, although, normally, a 5 to 10% accuracy improvement is expected (in average) after some habituation to the device.

Finally, it is regarded that all the proposed objectives for the project were achieved. The robot meets the desired reach and payload capacity while being relatively compact. From a manufacturing perspective, the 3D printed parts turned out not only with quite good accuracy and finishing but also as being quite robust. Lastly, the structural optimization allowed a 17% mass reduction on the conceived sprung components, which was considered a quite good accomplishment.

8.1. Future work

Although the robotic manipulator already delivers an overall acceptable performance, there are still some improvements that can be made. To what construction concerns, it is believed that the weight reduction of the sprung masses can be taken further by applying a more disruptive optimization approach or just by evaluating the possibility of not using a 100% infill density for printing and its side effects.

On the other hand, the experiments that have taken place were mostly for testing and having a notion of the real capabilities of the robot. Thereby, the next steps will probably be to investigate how it will operate in real specific tasks, for which, other tools can also be developed.

Regarding the software field, there is still some work to be made. First, a new control approach using the dynamic model of the robot will be implemented. Secondly, as the compliance of the actuators turned out underexplored, there is still some research that needs to be done. Lastly, there is the desire of taking experiments using Myo™ further, attempting to enhance its accuracy, developing an even better teamwork experience for the operator, and perhaps, trying to introduce new gestures or postures.

BIBLIOGRAPHY

- [1] U. Hagn *et al.*, “The DLR MIRO: A versatile lightweight robot for surgical applications,” *Ind. Rob.*, vol. 35, no. 4, pp. 324–336, 2008, doi: 10.1108/01439910810876427.
- [2] S. Popi and B. Miloradovi, “Light Weight Robot Arms – An overview,” vol. 14, no. March, pp. 818–822, 2015.
- [3] G. Hirzinger, A. Albu-Schäffer, M. Hähnle, I. Schaefer, and N. Sporer, “On a new generation of torque controlled light-weight robots,” *Proc. - IEEE Int. Conf. Robot. Autom.*, vol. 4, pp. 3356–3363, 2001, doi: 10.1109/robot.2001.933136.
- [4] N. Sporer, M. Hdmle, R. Krenn, a Pascucci, and M. Schedl, “DLR’s torque-controlled light weight robot,” *Mechatronics*, no. May, pp. 1710–1716, 2002.
- [5] R. Bischoff *et al.*, “The KUKA-DLR Lightweight Robot arm - A new reference platform for robotics research and manufacturing,” *Jt. 41st Int. Symp. Robot. 6th Ger. Conf. Robot. 2010, ISR/ROBOTIK 2010*, vol. 2, no. January, pp. 741–748, 2010.
- [6] A. Albu-Schäffer, S. Haddadin, C. Ott, A. Stemmer, T. Wimböck, and G. Hirzinger, “The DLR lightweight robot: Design and control concepts for robots in human environments,” *Ind. Rob.*, vol. 34, no. 5, pp. 376–385, 2007, doi: 10.1108/01439910710774386.
- [7] D. Busson and R. Bearee, “A Pragmatic Approach to Exploiting Full Force Capacity for Serial Redundant Manipulators,” *IEEE Robot. Autom. Lett.*, vol. 3, no. 2, pp. 888–894, 2018, doi: 10.1109/LRA.2018.2792541.
- [8] A. Albu-Schäffer, C. Ott, and G. Hirzinger, “A unified passivity based control framework for position, torque and impedance control of flexible joint robots,” *Springer Tracts Adv. Robot.*, vol. 28, pp. 5–21, 2007, doi: 10.1007/978-3-540-48113-3_2.
- [9] P. L. García, S. Crispel, E. Saerens, T. Verstraten, and D. Lefeber, “Compact Gearboxes for Modern Robotics: A Review,” *Front. Robot. AI*, vol. 7, p. 103, Aug. 2020, doi: 10.3389/frobt.2020.00103.
- [10] “COMPI - Robot Systems - Robotics Innovation Center - DFKI GmbH.”



- <https://robotik.dfki-bremen.de/en/research/robot-systems/compi.html> (accessed Apr. 25, 2021).
- [11] S. C. Gutiérrez, R. Zotovic, M. D. Navarro, and M. D. Meseguer, “Design and manufacturing of a prototype of a lightweight robot arm,” *Procedia Manuf.*, vol. 13, pp. 283–290, Jan. 2017, doi: 10.1016/j.promfg.2017.09.072.
- [12] A. Elfasakhany, E. Yanez, K. Baylon, and R. Salgado, “Design and Development of a Competitive Low-Cost Robot Arm with Four Degrees of Freedom,” *Mod. Mech. Eng.*, vol. 01, no. 02, pp. 47–55, 2011, doi: 10.4236/mme.2011.12007.
- [13] T. Liu, F. Guo, and Y. Yu, “Design of low-cost desktop robot based on 3D printing technology and open-source control system,” *Proc. 2019 IEEE 3rd Inf. Technol. Networking, Electron. Autom. Control Conf. ITNEC 2019*, no. Itnec, pp. 739–742, 2019, doi: 10.1109/ITNEC.2019.8729193.
- [14] R. Siemasz, K. Tomczuk, and Z. Malecha, “3D printed robotic arm with elements of artificial intelligence,” *Procedia Comput. Sci.*, vol. 176, no. October, pp. 3741–3750, 2020, doi: 10.1016/j.procs.2020.09.013.
- [15] R. Saerang *et al.*, “3D Printed 6-Axis Collaborative Arm Robot Using Force Limiting Feature for Service Robot,” *IOP Conf. Ser. Earth Environ. Sci.*, vol. 426, no. 1, 2020, doi: 10.1088/1755-1315/426/1/012135.
- [16] A. De Luca, A. Albu-Schäffer, S. Haddadin, and G. Hirzinger, “Collision detection and safe reaction with the DLR-III lightweight manipulator arm,” *IEEE Int. Conf. Intell. Robot. Syst.*, pp. 1623–1630, 2006, doi: 10.1109/IROS.2006.282053.
- [17] S. Haddadin, S. Parusel, R. Belder, A. Albu-Schäffer, and G. Hirzinger, “Safe acting and manipulation in human environments: A key concept for robots in our society,” *Proc. IEEE Work. Adv. Robot. its Soc. Impacts, ARSO*, no. January, pp. 72–75, 2011, doi: 10.1109/ARSO.2011.6301962.
- [18] J. Saenz *et al.*, “Methods for considering safety in design of robotics applications featuring human-robot collaboration,” *Int. J. Adv. Manuf. Technol.*, vol. 107, no. 5–6, pp. 2313–2331, 2020, doi: 10.1007/s00170-020-05076-5.
- [19] “ISO - ISO 10218-1:2011 - Robots and robotic devices — Safety requirements for industrial robots — Part 1: Robots,” 2011. <https://www.iso.org/standard/51330.html> (accessed Apr. 21, 2021).
- [20] “ISO - ISO 10218-2:2011 - Robots and robotic devices — Safety requirements for

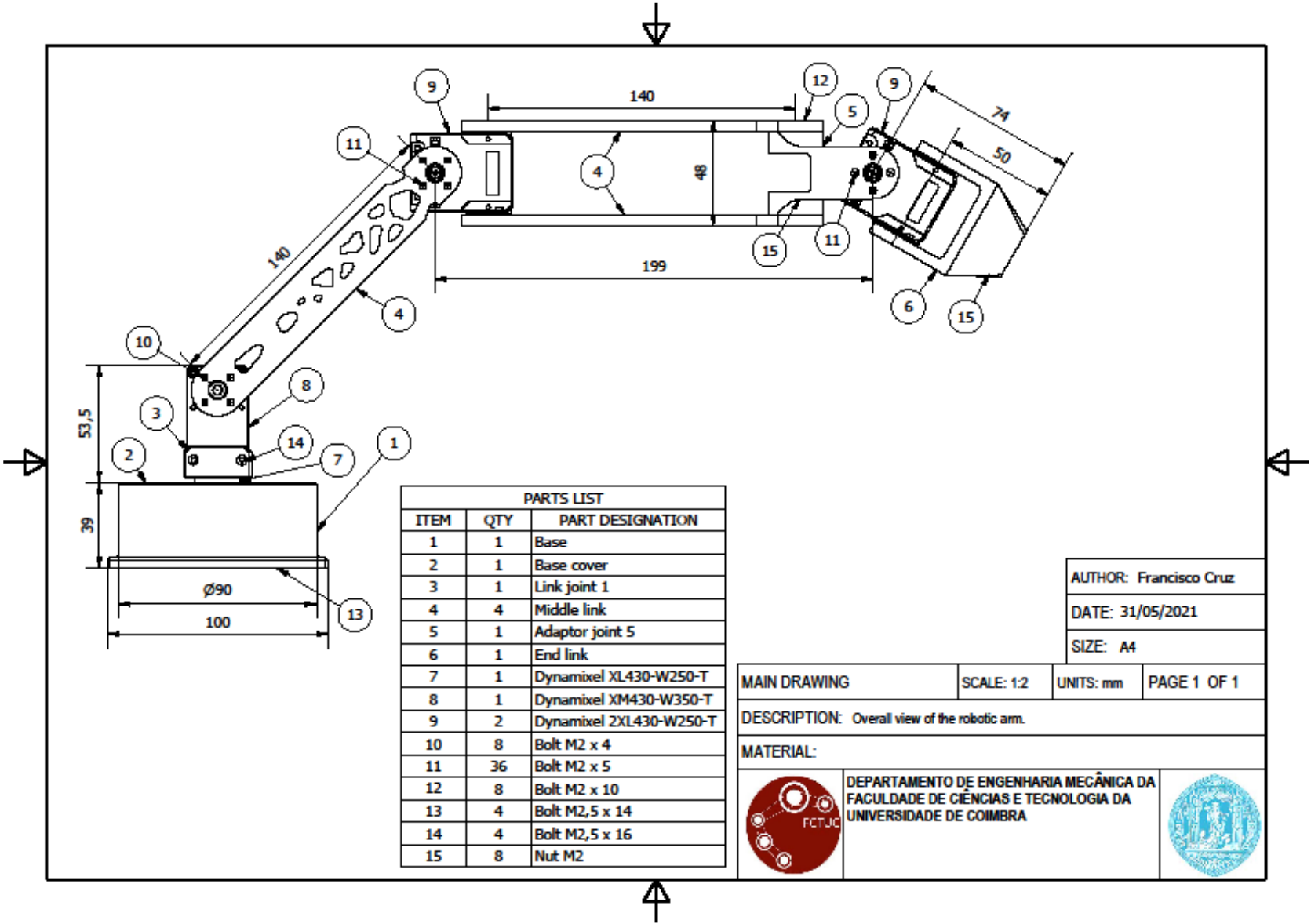
-
- industrial robots — Part 2: Robot systems and integration.”
<https://www.iso.org/standard/41571.html> (accessed Apr. 21, 2021).
- [21] A. W. Gebisa and H. G. Lemu, “A case study on topology optimized design for additive manufacturing,” *IOP Conf. Ser. Mater. Sci. Eng.*, vol. 276, no. 1, 2017, doi: 10.1088/1757-899X/276/1/012026.
- [22] S. Junk, B. Klerch, and U. Hochberg, “Structural optimization in lightweight design for additive manufacturing,” *Procedia CIRP*, vol. 84, pp. 277–282, 2019, doi: 10.1016/j.procir.2019.04.277.
- [23] K. Cheng, Y. Liu, R. Wang, J. Zhang, and X. Jiang, “Journal of the Mechanical Behavior of Biomedical Materials Topological optimization of 3D printed bone analog with PEKK for surgical mandibular reconstruction,” vol. 107, no. April, 2020.
- [24] “2XL430-W250-T.” <https://emmanual.robotis.com/docs/en/dxl/x/2xl430-w250/> (accessed Apr. 27, 2021).
- [25] “XM430-W350-T/R.” <https://emmanual.robotis.com/docs/en/dxl/x/xm430-w350/> (accessed Apr. 27, 2021).
- [26] “XL430-W250-T.” <https://emmanual.robotis.com/docs/en/dxl/x/xl430-w250/> (accessed Apr. 27, 2021).
- [27] “3D Printed Mini Robotic Gripper (TfCD) : 5 Steps (with Pictures) - Instructables.” <https://www.instructables.com/3D-Printed-Mini-Robotic-Gripper/> (accessed Apr. 20, 2021).
- [28] P. Neto, M. Simão, N. Mendes, and M. Safeea, “Gesture-based human-robot interaction for human assistance in manufacturing,” *Int. J. Adv. Manuf. Technol.*, vol. 101, no. 1–4, pp. 119–135, 2019, doi: 10.1007/s00170-018-2788-x.
- [29] U. Muhammad, K. A. Sipra, M. Waqas, and S. Tu, “Applications of Myo Armband Using EMG and IMU Signals,” *2020 3rd Int. Conf. Mechatronics, Robot. Autom. ICMRA 2020*, no. October, pp. 6–11, 2020, doi: 10.1109/ICMRA51221.2020.9398375.
- [30] “Myo SDK MATLAB MEX Wrapper - File Exchange - MATLAB Central.” <https://www.mathworks.com/matlabcentral/fileexchange/55817-myo-sdk-matlab-mex-wrapper> (accessed Jun. 13, 2021).
-

APPENDIX A (MANIPULATOR TECHNICAL DRAWINGS)

Technical drawing showing an exploded view of a robotic arm assembly. The drawing includes 15 numbered callouts (1-15) pointing to various components. The assembly consists of a base (1), base cover (2), two middle links (4), an adaptor joint (5), and an end link (6). It also features two Dynamixel XL430-W250-T (7) and one Dynamixel XM430-W350-T (8) motors. The assembly is secured with various bolts (10, 11, 12, 13, 14) and nuts (15).

PARTS LIST		
ITEM	QTY	PART DESIGNATION
1	1	Base
2	1	Base cover
3	1	Link joint 1
4	4	Middle link
5	1	Adaptor joint 5
6	1	End link
7	1	Dynamixel XL430-W250-T
8	1	Dynamixel XM430-W350-T
9	2	Dynamixel 2XL430-W250-T
10	8	Bolt M2 x 4
11	36	Bolt M2 x 5
12	8	Bolt M2 x 10
13	4	Bolt M2,5 x 14
14	4	Bolt M2,5 x 16
15	8	Nut M2

AUTHOR: Francisco Cruz			
DATE: 31/05/2021			
SIZE: A4			
ASSEMBLY DRAWING	SCALE: 1:2	UNITS: mm	PAGE 1 OF 1
DESCRIPTION: Assembly view of the robotic arm.			
MATERIAL:			
	DEPARTAMENTO DE ENGENHARIA MECÂNICA DA FACULDADE DE CIÊNCIAS E TECNOLOGIA DA UNIVERSIDADE DE COIMBRA		





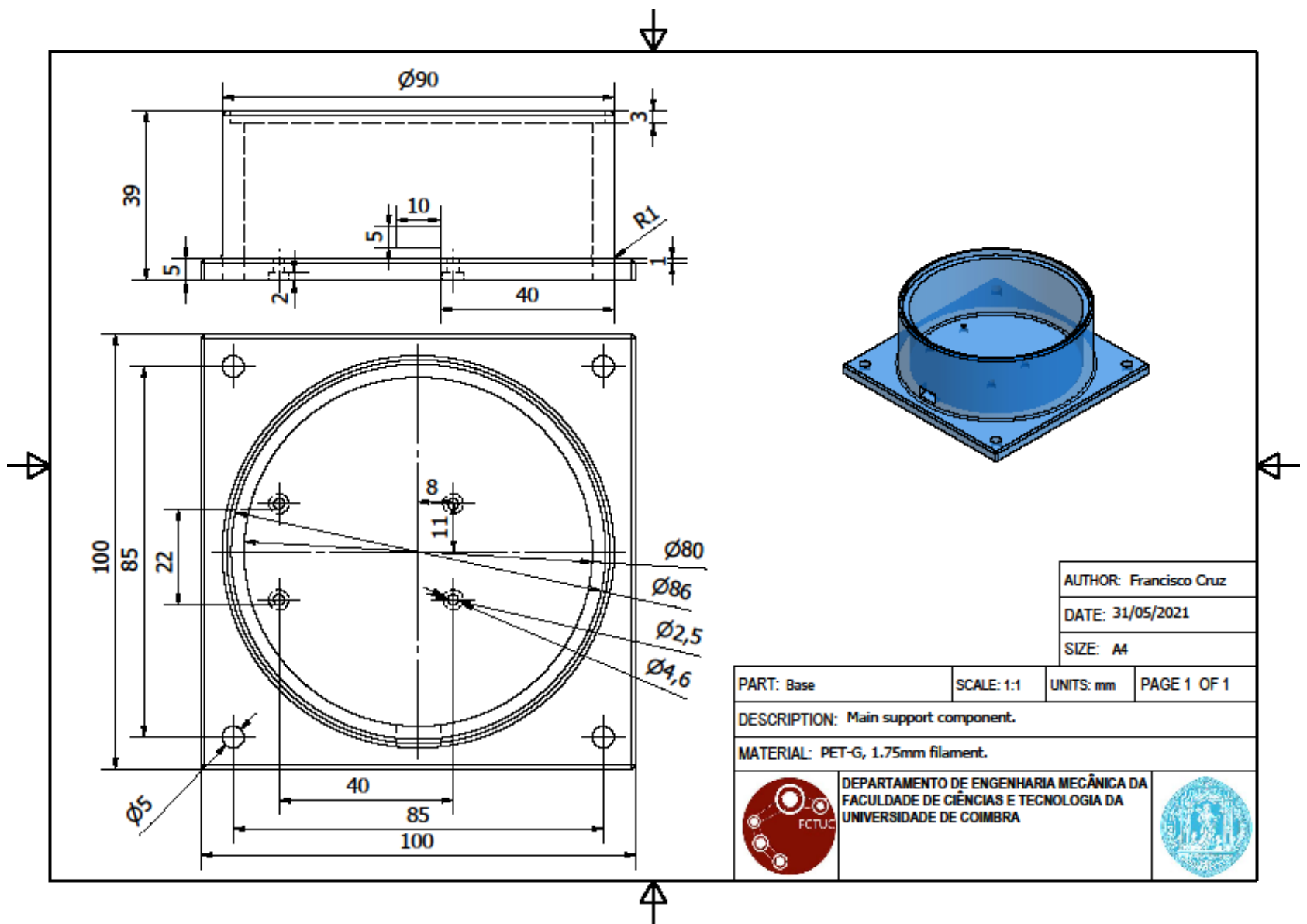
AUTHOR: Francisco Cruz
 DATE: 31/05/2021
 SIZE: A4

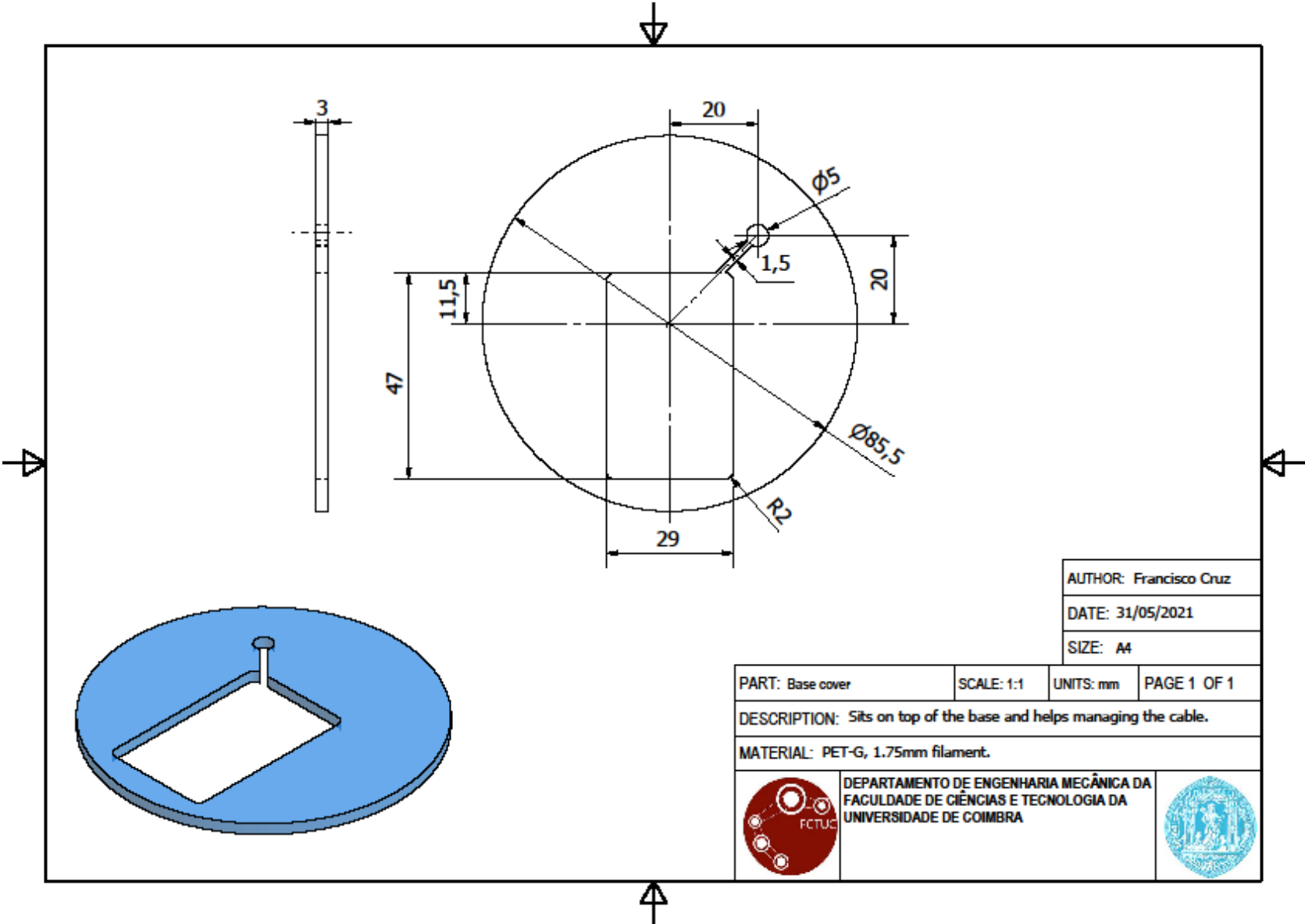
MAIN DRAWING SCALE: 1:2 UNITS: mm PAGE 1 OF 1

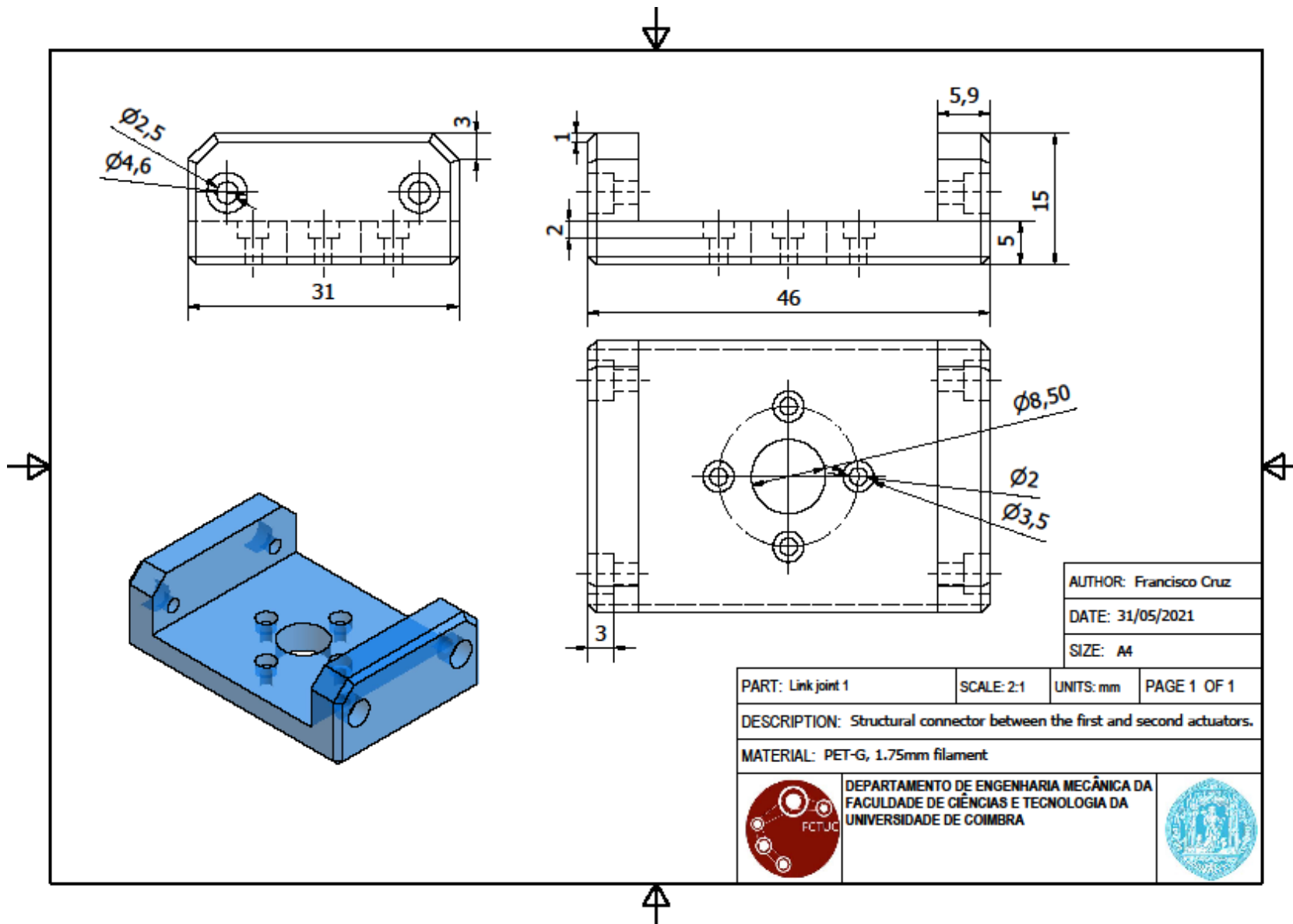
DESCRIPTION: Overall view of the robotic arm.

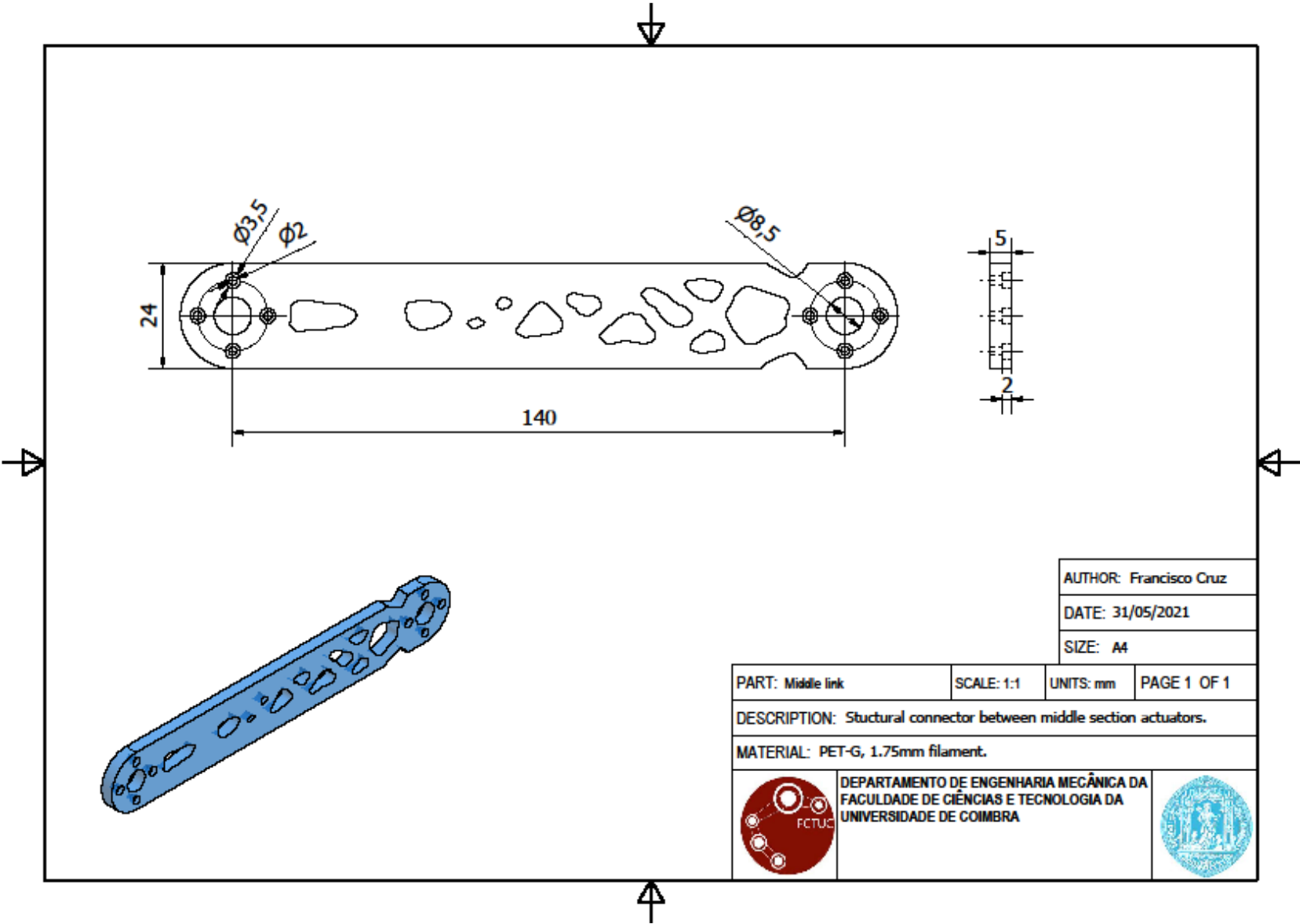
MATERIAL:

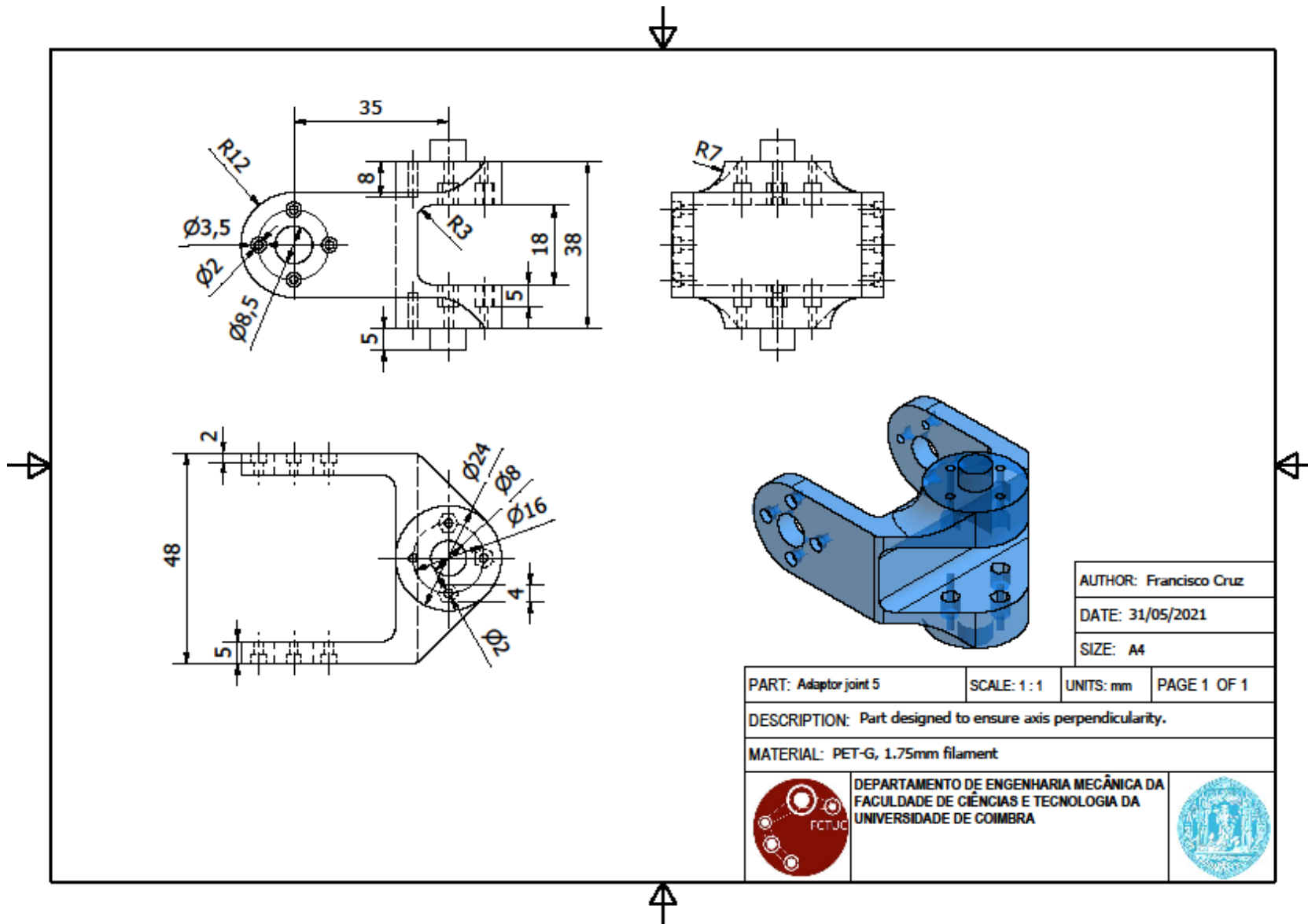

 DEPARTAMENTO DE ENGENHARIA MECÂNICA DA
 FACULDADE DE CIÊNCIAS E TECNOLOGIA DA
 UNIVERSIDADE DE COIMBRA
 













AUTHOR: Francisco Cruz
 DATE: 31/05/2021
 SIZE: A4

PART: Adaptor joint 5 SCALE: 1 : 1 UNITS: mm PAGE 1 OF 1

DESCRIPTION: Part designed to ensure axis perpendicularity.

MATERIAL: PET-G, 1.75mm filament

	DEPARTAMENTO DE ENGENHARIA MECÂNICA DA FACULDADE DE CIÊNCIAS E TECNOLOGIA DA UNIVERSIDADE DE COIMBRA	
---	--	---

